

6-1977

The Effect of Solvent Polarity on the S1-T2 Energy Gap in 9- and 2-Substituted Anthracene Derivatives in Aromatic and Non-Aromatic Solvents

John S. Facci

Union College - Schenectady, NY

Follow this and additional works at: <https://digitalworks.union.edu/theses>

 Part of the [Chemistry Commons](#)

Recommended Citation

Facci, John S., "The Effect of Solvent Polarity on the S1-T2 Energy Gap in 9- and 2-Substituted Anthracene Derivatives in Aromatic and Non-Aromatic Solvents" (1977). *Honors Theses*. 1858.
<https://digitalworks.union.edu/theses/1858>

This Open Access is brought to you for free and open access by the Student Work at Union | Digital Works. It has been accepted for inclusion in Honors Theses by an authorized administrator of Union | Digital Works. For more information, please contact digitalworks@union.edu.

THE EFFECT OF SOLVENT POLARITY ON THE S_1 - T_2 ENERGY
GAP IN 9- AND 2-SUBSTITUTED ANTHRACENE DERIVATIVES
IN AROMATIC AND NON-AROMATIC SOLVENTS

by

Typed
John S. Facci 10/19/77

Submitted in partial fulfillment
of the requirements for
Honors in the Department of Chemistry

UNION COLLEGE

April, 1977

3
JAN 1970
FISKE
1977
C.2

ABSTRACT

Fluorescence quantum yields, fluorescence lifetimes, S_1 energies and intersystem crossing activation energies were measured for methyl-2-anthroate and methyl-9-anthroate in various polar, non-polar and aromatic solvents. Methyl-2-anthroate shows an increase in quantum yield and activation energy with increasing solvent polarity while methyl-9-anthroate shows a decrease in quantum yield and increase in activation energy with increasing solvent polarity. These results are interpreted in terms of a vibrational structuring of the Franck-Condon factor when the lowest excited singlet state and accepting triplet lie close in energy.

Weak π - π solute-solvent interaction has been found between aromatic solvents and methyl-2-anthroate and methyl-9-anthroate. This interaction has been inferred from red-shifted S_1 and T_2 energies for these molecules in aromatic solvents and from an increase in activation energy with increasing temperature for these molecules in a given aromatic solvent.

DEDICATION

I would like to dedicate this work to Sam Casella and Marianne Ross whose friendship and encouragement made my four years at Union interesting and enjoyable, and to Lisa D'Arezzo, a fellow anthracene photochemist.

ACKNOWLEDGMENT

I would like to thank the Petroleum Research Fund for providing financial support for this project. The many enlightening discussions and help in the preparation of this manuscript by Dr. T. C. Werner is also gratefully acknowledged.

John S. Facci
John S. Facci

Hold fast to dreams
For if dreams die
Life is a broken-winged bird
That cannot fly.

Hold fast to dreams
For when dreams go
Life is a barren field
Frozen with snow.

Langston Hughes

TABLE OF CONTENTS

| | <u>Page</u> |
|-----------------------------|-------------|
| ABSTRACT | ii |
| DEDICATION | iii |
| ACKNOWLEDGEMENT | iv |
| QUOTE | v |
| STRUCTURE OF COMPOUNDS USED | x |
| INTRODUCTION | 1 |
| EXPERIMENTAL | 24 |
| RESULTS | 40 |
| DISCUSSION | 51 |
| FUTURE WORK | 101 |
| REFERENCES | 104 |

INDEX OF TABLES AND FIGURES

I. Figures

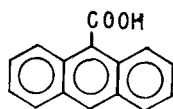
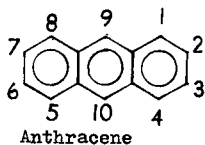
| <u>Number</u> | <u>Title</u> | <u>Page</u> |
|---------------|--|-------------|
| 1 | Jablonski Diagram | 2 |
| 2 | Franck-Condon Jablonski Diagram | 16 |
| 3 | Relationship Between E_a and the Singlet-Triplet Energy Gap | 21 |
| 4 | Wavelength Correction Curve for Cary 118C | 29 |
| 5 | Thermocouple-Voltmeter Temperature Correction Curve | 35 |
| 6 | Temperature Controlled Silicone Oil Bath Used in the Polymerization of Polymethylmethacrylate | 37 |
| 7a | ϕ_f vs. Temperature for 9-COOMe in Benzene, Toluene and Benzonitrile | 46 |
| 7b | ϕ_f vs. Temperature for 2-COOMe in Benzonitrile | 48 |
| 8 | Fluorescence Rate Constants for 9-COOMe and 2-COOMe as a Function of Solvent Polarity | 56 |
| 9 | Arrhenius Plots for 9-COOMe in Ethanol, Methanol and p-Dioxane | 60 |
| 10 | Fluorescence Quantum Yield as a Function of Solvent Polarity for 9-COOMe | 65 |
| 11 | 9-COOMe S_1 Energy vs. Solvent Polarity | 68 |
| 12 | Electronic Distribution in the Excited State (S_1) of 9-COOMe and Partial Structure of the Solvent Cage and Exciplex | 73 |
| 13 | Activation Energy as a Function of Solvent Polarity for 9-COOMe | 75 |
| 14 | S_1 Energy + E_a for 9-COOMe as a Function of Solvent Polarity | 79 |

| <u>Number</u> | <u>Title</u> | <u>Page</u> |
|---------------|---|-------------|
| 15 | Activation Energy vs. S_1 Energy for 9-COOMe | 83 |
| 16 | S_1 Energy vs. Solvent Polarity for 2-COOMe | 85 |
| 17 | $S_1 + E_a$ vs. Solvent Polarity for 2-COOMe | 89 |
| 18 | ϕ_f vs. Solvent Polarity for 2-COOMe | 93 |

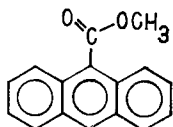
II. Tables

| <u>Number</u> | <u>Title</u> | <u>Page</u> |
|---------------|--|-------------|
| 1 | Wavelength Correction Factors for the Cary 118C | 28 |
| 2 | Absorption and Fluorescence Energies, Fluorescence Quantum Yields for Esters of 9- and 2-Anthroic Acid in Various Solvents | 41 |
| 3 | Fluorescence Lifetimes and Activation Energies for 2-COOMe and 9-COOMe in Various Solvents | 44 |
| 4 | Fluorescence Rate Constants and Activation Energy for 9-COOMe and 2-COOMe | 55 |
| 5 | Intersystem Crossing Rate Constants for 9-COOMe and 2-COOMe in Various Solvents | 64 |
| 6 | $S_1 + E_a$ for 9-COOMe and 2-COOMe in Aromatic and Non-aromatic Solvents | 78 |

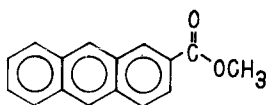
STRUCTURES OF COMPOUNDS USED



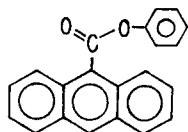
9-Anthroic acid



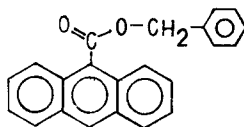
Methyl-9-anthroate



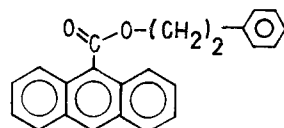
Methyl-2-anthroate



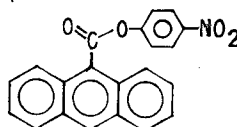
Phenyl-9-anthroate



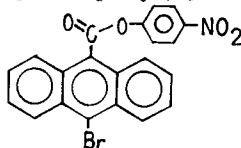
Benzyl-9-anthroate



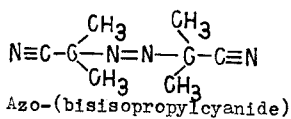
(β -Phenylethyl)-9-anthroate



(p-Nitrophenyl)-9-anthroate



10-Bromo-9-(p-nitrophenyl)-anthroate



INTRODUCTION

INTRODUCTION

Aromatic and polynuclear aromatic molecules have electronic energy levels which can be populated by the absorption of light in the near ultraviolet and visible spectrum. One of the ways in which these molecules may lose the excess energy gained by absorption of a photon is to reemit that energy in a process called fluorescence. Another radiative process by which excited state energy may be lost is known as phosphorescence.

A Jablonski Diagram shown in Figure 1 indicates the salient features of the absorption process and the processes through which the molecule loses energy from its excited state. The following mechanisms are generally accepted to hold.

| | | | |
|------|----------------------------------|-------------------|----------------------|
| 1(a) | $1_A \xrightarrow{h\nu} 1_A^*$, | I_a | Absorption |
| (b) | $1_A^* \rightarrow 1_A + h\nu$, | $k_f [1_A^*]$ | Fluorescence |
| (c) | $1_A^* \rightarrow 1_A$, | $k_{ic} [1_A^*]$ | Internal Conversion |
| (d) | $1_A^* \rightarrow 3_A^*$, | $k_{isc} [1_A^*]$ | Intersystem Crossing |
| (e) | $3_A^* \rightarrow 1_A + h\nu$, | $k_p [3_A^*]$ | Phosphorescence |

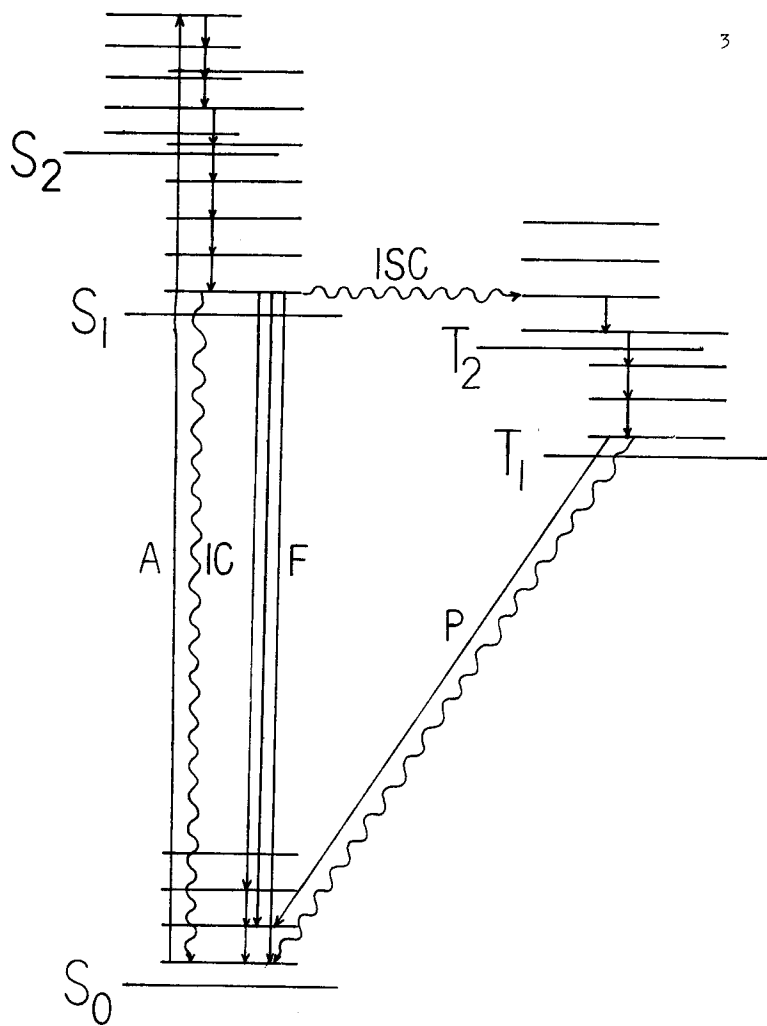
The superscripts refer to the multiplicity of the molecule and the star refers to the molecule in an excited state.

Prior to excitation, the molecule is usually in the lowest vibrational level in its singlet ground electronic state (S_0). Absorption of a photon of the proper energy (A) causes excitation to one of the vibrational levels of an excited state (S_1, S_2, S_3, \dots). The molecule then rapidly undergoes

Figure I

Jablonski Diagram

Following absorption of light (A), the molecule undergoes rapid electronic and/or vibrational relaxation to the lowest vibrational level of S_1 , the lowest excited singlet state. Fluorescence (F), a radiative process and internal conversion (IC), a non-radiative process, deactivate the molecule from S_1 to S_0 . Intersystem crossing (ISC), a non-radiative process, may occur to the triplet state from which either phosphorescence (P) or another radiationless intersystem crossing process may occur to S_0 .



vibrational relaxation to the 0th vibrational level of S_1 . The rate constant for this process is on the order of 10^{11} to 10^{12} sec^{-1} (1). If the molecule is excited to a state higher in energy than S_1 , electronic relaxation must occur as well as vibrational relaxation. Electronic relaxation occurs readily when the energy separation is small and when one of the vibrational levels of the more energetic state is isoenergetic and has the same symmetry properties as a vibrational level in a lower state of the same multiplicity. It is believed that this isoenergetic vibronic transition between electronic states of the same multiplicity is the rate determining step when vibrational relaxation occurs. The rationale for extremely rapid vibronic relaxation lies in the fact that fluorescence (F) is observed to occur almost exclusively from the lowest vibrational level of the first excited singlet. One interesting exception is the observation of fluorescence from S_2 in [18] annulenes (2) presumably because the energy gap between S_1 and S_2 is large ($14,000 \text{ cm}^{-1}$) and the symmetry of the two states are not compatible. The energy of the photon emitted during fluorescence is equal to the energy difference between the lowest vibrational level of S_1 and one of the vibrational levels of S_0 and hence vibrational structure is often observed in the emission spectrum of fluorescent molecules. This accounts for the highly structured fluorescence spectrum of anthracene and methyl-2-anthroate in non-polar solvents. Once the

molecule is in one of the vibrational levels of S_0 , rapid vibrational relaxation occurs to the 0th vibrational level. Fluorescence rate constants (k_f) are typically on the order of 10^7 to 10^9 sec^{-1} (1).

S_1 may also be depopulated through a non-radiative pathway called internal conversion (IC) in which energy is usually transferred to the solvent environment. Another non-radiative process which depopulates S_1 is known as intersystem crossing (ISC). The rate constant for internal conversion (k_{ic}) in anthracene and its derivatives is typically on the order of 10^5 to 10^7 sec^{-1} (1), while the intersystem crossing rate constant (k_{isc}) for these molecules may vary from 10^5 to 10^8 sec^{-1} (1). Intersystem crossing occurs when one of the vibrational levels of S_1 is isoenergetic with a vibrational level of a nearby triplet (T_X , $X = 1, 2, 3, \dots$). Upon entering the triplet manifold, the molecule undergoes vibrational and electronic relaxation to the 0th vibrational level of T_1 . Return to S_0 from T_1 may occur by either phosphorescence (a radiative pathway) or another radiationless intersystem crossing process, $T_1 \rightarrow S_0$. Phosphorescence rate constants are usually on the order of 10^3 to 10^{-1} sec^{-1} (1).

State multiplicities determine the rate at which emission processes occur. Quantum mechanics predicts that highly probable transitions will occur only when the change in spin states is zero, i.e. transitions occur between states of the same multiplicity. When the change in spin states is greater

than zero, the probability of the transition is zero and hence the transition is forbidden. This condition is true only when the electronic states are "pure" and have no contributions from other electronic states of different multiplicity in their wavefunctions. Hence singlet to triplet and triplet to singlet transitions are theoretically predicted to be forbidden. However, in actual fact transitions between states of different multiplicities do occur because of state mixing which is thought to occur through vibronic coupling and spin-orbit coupling. The wavefunction of a singlet state may have a small contribution from a triplet state (not necessarily a triplet involved in a transition with the singlet state) and hence mixing is said to occur making the probability nonzero. Therefore the probability of the $S_0 \rightarrow T_1$ transition is some very low but finite value making it a very difficult to measure, low intensity transition. This transition has not been observed for methyl-2-anthroate even in concentrated solutions in methylene iodide (1 cm cell) where the presence of the heavy atom, iodine, is thought to increase the probability of the transition through enhanced spin-orbit coupling. Similarly the process $T_1 \rightarrow S_0$ is also forbidden but does occur under the proper conditions (rigid matrix) and has been measured for anthracene in polymethylmethacrylate. Attempts to measure the phosphorescence of methyl-2-anthroate have not succeeded. Because of the forbiddenness of the transition, phosphorescence

lifetimes are very long (10^{-3} to 10^0 sec) and hence internal conversion from T_1 to S_0 can often compete successfully with phosphorescence making phosphorescence very difficult to measure in anthracene and its derivatives.

Radiationless transitions such as internal conversion and intersystem crossing are of considerable theoretical interest. Franck-Condon factors are often invoked to explain the probabilities and rate constants for non-radiative transitions(3,4,5,6). To a first approximation, when the electronic state energy difference is very large, the vibrational overlap integral (Franck-Condon factor) becomes very small and hence the probability of transition becomes very low(3). If the energy difference is small, the Franck-Condon factor may be quite large (approximately one) and the transition probability is correspondingly higher. In this latter case, it is interesting that actual crossing of the electronic state potential surfaces (the existence of a classical crossing point) is not necessary as the vibrational wavefunctions extend beyond the potential surface. Hence it is not expected that tunnelling is not a requirement when the electronic states are close in energy.

In general, the rate constant for a radiationless transition is a function of the symmetry characteristics of the vibrational levels involved, the density of states at a given energy and various quantum mechanical considerations which can be neglected for the moment, as well as the Franck-Condon

factor⁽³⁾. Consider the internal conversion from S_1 to S_0 . The number of vibrational levels of S_0 at S_1 is referred to as the density of states of S_0 at S_1 . This is primarily a function of the number of fundamental vibrational modes for the molecule, which is 84 in the case of methyl-9-anthroate, the energies of these modes and the electronic energy difference. The density of states at a given energy level is the total number of combinations of vibrational energy levels which when added to the electronic energy of S_0 will give an energy level in S_1 . Obviously, the greater the number of fundamental modes and the greater the electronic energy difference, the greater the density of states. The density of states of S_0 at S_1 in methyl-9-anthroate is exceedingly high and approaches that of a continuum⁽³⁾. However, the Franck-Condon factors for the energy difference in this molecule ($22,000 \text{ cm}^{-1}$) are very low as is the probability that any of the states of S_0 at the S_1 energy will have the proper symmetry to promote a radiationless transition from S_1 to S_0 . Which of these factors dominates must be determined from experimental data which are presented later.

In general any non-radiative transition can be broken down into two steps. The first involves the transition between two isoenergetic vibrational levels of different electronic states and the second involves vibrational relaxation within the lower electronic state. Because of certain quantum considerations, the first step is thought to be rate determining⁽²⁾

and hence the rate constant is expressed as shown below in equation (2),

$$k_{NR} = CV^2F\rho \quad (2)$$

where C is a constant, V is an electronic matrix element which allows crossing between different electronic states, F is the Franck-Condon factor and ρ is the density of states. For the purposes of this work, changes in V can be neglected. Equation (2) shows that as expected the non-radiative rate constant, k_{NR} , is directly proportional to the Franck-Condon factor and the density of states.

As will be shown later the $S_1 \rightarrow T_1$ transition in anthracene and its derivatives involves an energy gap on the order of $10,000 \text{ cm}^{-1}$. For the same reasons that $S_1 \rightarrow S_0$ internal conversion is not expected to occur, the $S_1 \rightarrow T_1$ intersystem crossing process is probably not important, although experimental evidence is needed to support this. Data for singlet-triplet energy gaps⁽³⁾ for various polynuclear aromatic hydrocarbons indicate that when the gap is large ($\sim 10,000 \text{ cm}^{-1}$), the non-radiative rate constant can be as low as 10^4 sec^{-1} , but that when the energy gap is small, as in intersystem crossing, the non-radiative rate constant can be as large as 10^7 sec^{-1} which is comparable with k_F . Because of the large $S_1 \rightarrow T_1$ energy gap in methyl-2-anthroate and methyl-9-anthroate, the non-radiative rate constant for this $S_1 \rightarrow T_1$ transition in almost all solvents may be too low to compete successfully with k_F . With this large energy gap, the Franck-Condon factor

is small but the density of states is large while in the case of the small energy gap the Franck-Condon factor is large but the density of states is low. Hence it appears that from the above data, non-radiative constants are more affected by Franck-Condon factors than the density of states.

The number of photons emitted through fluorescence divided by the number of photons absorbed is called the fluorescence quantum yield (ϕ_f). This quantity can also be expressed in terms of the rate constants for the three processes described above which depopulate S_1 : k_f , k_{isc} , k_{ic} . At any temperature, ϕ_f is equal to the ratio of the rate constant of fluorescence and the sum of the rate constants for all of the processes which depopulate S_1 (equation 3).

$$\phi_f = k_f / (k_f + k_{isc} + k_{ic}) \quad (3)$$

The measurement of lifetime of the first excited singlet can be carried out using a pulsed nanosecond flash technique. A pulsed nanosecond nitrogen laser is used to excite the fluorescent molecule into its first excited state and the decay of the intensity of fluorescence is recorded versus time. The time required for the intensity to fall to e^{-1} of its initial value is called the fluorescence lifetime (τ_f) and can be expressed in terms of the processes deactivating S_1 (equation 4)

$$\tau_f = 1 / (k_f + k_{isc} + k_{ic}) \quad (4)$$

The expression for τ_f is valid at any temperature and hence equation 4 can be combined with equation 3 to give an alternate

expression for the fluorescence quantum yield in terms of the rate constant and lifetime of fluorescence (equation 5).

$$\phi_f = k_f \tau_f \quad (5)$$

There are many indications that k_f is independent of temperature for a particular molecule. Studies of the variability of k_f as a function of temperature⁽⁷⁾ on anthracene indicate only a very slight temperature dependence. The fluorescence rate constant is similarly seen to be independent of solvent effects. Work done by Hawkins⁽⁸⁾ and Matthews⁽⁹⁾ and the present work indicate that k_f is fairly independent of solvent in non-polar, aromatic and polar solvents. Hence k_f is seen as a molecular property not greatly dependent on the effects of temperature or solvent.

Measurements of the temperature dependence of fluorescence quantum yields show a decrease in ϕ_f with increasing temperature for methyl-2-anthroate and methyl-9-anthroate. Changes in solvent polarity also affect ϕ_f . Methyl-2-anthroate shows a maximum in ϕ_f with increasing solvent polarity. On the other hand, methyl-9-anthroate shows a monotonic decrease in ϕ_f with increasing solvent polarity. In addition methyl-9-anthroate shows a greater variation in ϕ_f than methyl-2-anthroate over the same range of polarity increasing from less than 0.1 in methanol to almost 0.9 in cyclohexane.

Since, as discussed above, the variation in ϕ_f cannot be a result of changes in k_f , it must come about as a result of variations in k_{isc} or k_{ic} or both. The process of internal

conversion from S_1 to S_0 involves energy gaps of roughly 21,000 and 24,000 cm^{-1} for methyl-9-anthroate and methyl-2-anthroate, respectively, while intersystem crossing involves energy changes of less than 3000 cm^{-1} (10). Where small energy gaps are involved the Franck-Condon factor (degree of vibrational overlap) is dominated by skeletal vibrations but in the case of large energy gaps, these factors are dominated by C-H vibrations⁽³⁾. Hence deuteration would affect only the Franck-Condon factor for large energy differences such as those between S_0 and S_1 and we would expect that the rate constant for internal conversion from S_1 in anthracene and its derivatives would be considerably affected. Because C-D vibrations are of lower energy than C-H vibrations, higher vibrational levels would be involved in $S_1 \rightarrow S_0$ internal conversion in the perdeuterated compound, which results in a higher density of vibrational states of S_0 at S_1 but in a lower Franck-Condon factor. Hence k_{ic} should decrease with deuteration while k_{isc} is not expected to be affected and from equations 4 and 5, τ_f and ϕ_f will show an increase only if k_{ic} is of the same magnitude as k_f . Extensive deuteration studies have been performed on a wide variety of aromatic and polynuclear aromatic compounds⁽¹¹⁾. The results of these studies show that the fluorescence lifetimes and hence fluorescence quantum yields of the perhydro and perdeutero derivatives of the same parent compound are virtually the same. Additional evidence for the absence of

internal conversion in anthracene derivatives has come from flash work done by Horrocks⁽¹⁷⁾. Therefore internal conversion to S_0 occurs to a negligible extent ($k_{ic} \ll k_f$). Hence we postulate that intersystem crossing is the temperature dependent process responsible for the temperature dependence and solvent dependence of ϕ_f in methyl-2-anthroate and methyl-9-anthroate. If our postulate is correct then intersystem crossing and fluorescence are the only processes of importance which depopulate S_1 in these molecules.

Because intersystem crossing may be responsible for the solvent and temperature dependence of ϕ_f , a consideration of the properties of S_1 and the accepting triplet is important. Our evidence tends to show that S_1 is a more polar state than S_0 in both methyl-2-anthroate⁽⁸⁾ and methyl-9-anthroate. It was found that with increasing solvent polarity, the fluorescence spectrum of these molecules shows a substantial red shift over the range of solvent polarity used. This results in S_1 (strictly speaking, the equilibrium excited state shown later in Figure 2) dropping in energy and a decreasing energy difference between S_1 and S_0 . The energy of the first triplet (T_1) can be measured through phosphorescence studies. Unfortunately T_1 has not been measured for methyl-2-anthroate and methyl-9-anthroate because the intensity of phosphorescence is extremely low. However, a reasonable approximation of T_1 in these molecules would be $14,700 \text{ cm}^{-1}$ which is the value of T_1 in anthracene. It has been shown that the triplet

manifold of the parent anthracene is relatively insensitive to substitution⁽¹²⁾ and solvent polarity⁽¹³⁾. Hence T_1 and higher energy triplets are expected to remain fairly constant relative to S_0 and relatively independent of the environment. The energy of these higher energy triplets may be located through triplet-triplet absorption measurements. Several triplets have been predicted to be near $26,700 \text{ cm}^{-1}$ in anthracene and one has been found at $26,050 \text{ cm}^{-1}$ (14) and $26,000 \text{ cm}^{-1}$ (15) in anthracene- d_{10} . It is generally assumed that this triplet is T_2 and that the T_2 state is the one involved in intersystem crossing in methyl-9-anthroate and methyl-2-anthroate. Additional evidence has been found in pressure dependent studies of S_1 and T_2 in anthracene that show that the energy of T_2 is considerably less affected by environmental effects than S_1 . Shaw⁽¹⁵⁾ has found that the energy of S_1 relative to S_0 in anthracene- d_{10} decreases 4-5 times faster than that of T_2 relative to S_0 with increases in pressure applied to solutions of this molecule in polymethylmethacrylate.

T_1 is considered to be too far below S_1 to have any effect on k_{isc} . Results for perdeuterated 9-methylanthracene indicate that the C-H vibrations are not expected to play an important role in intersystem crossing⁽¹⁶⁾ indicating the existence of a small S_1-T_X energy gap where T_X is the accepting triplet. Therefore T_X is higher than the lowest one and is probably T_2 . Hence we postulate that S_1 is below T_2 in both the 9- and 2-methyl esters above since no direct spectral

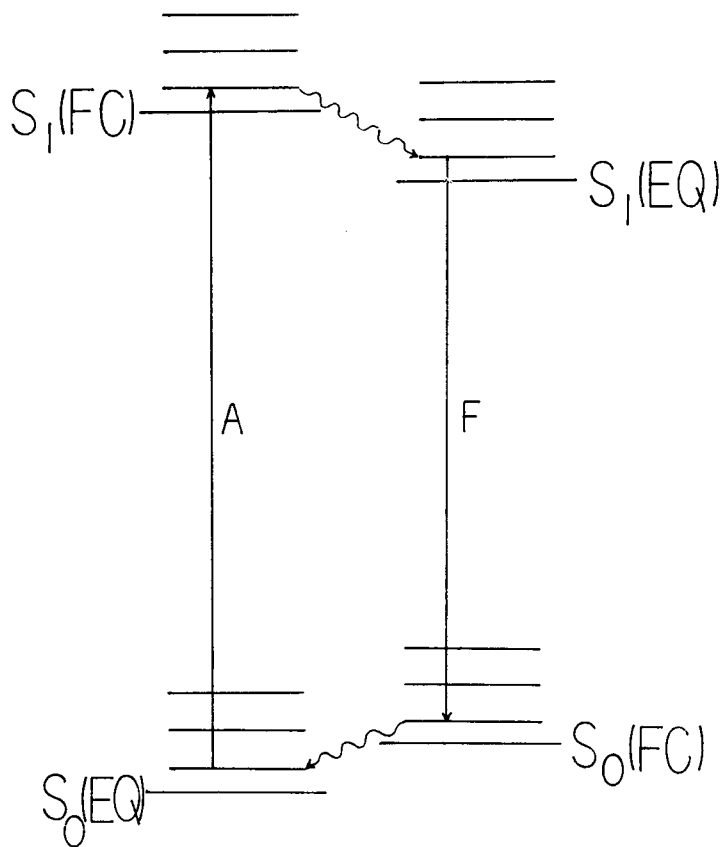
evidence exists which gives the energies of T_1 and T_2 . It is known, however, that the S_1 energy in the 9-ester lies below that of the 2-ester. A scheme of energy levels for methyl-2-anthroate has been proposed by Hawkins⁽⁸⁾ which accounts for the increasing ϕ_f with increasing solvent polarity, but this model does not explain well the maximum which ϕ_f for methyl-2-anthroate exhibits with increasing solvent polarity since internal conversion is fairly well established to be negligible in polynuclear aromatic hydrocarbons and since k_{isc} is probably very low for the $S_1 \rightarrow T_1$ transition. In addition, this model does not explain at all the unexpected trend of a decreasing ϕ_f with increasing solvent polarity for the 9-ester.

Since the relative energy of S_1 is important in inter-system crossing, an examination of the Franck-Condon principle as it applies to S_1 is necessary. The Franck-Condon principle states that electronic motion (10^{-15} sec) is much faster than nuclear motion (10^{-12} sec). Immediately after excitation, the molecule is in the Franck-Condon excited state, $S_1(FC)$, and undergoes rapid vibrational relaxation (Figure 2). A molecule in this state has the ground state molecular and solvent cage geometry. As stated previously, the lifetime of S_1 is on the order of 10^{-7} - 10^{-9} sec during which there is ample time for the solvent cage to rearrange to accommodate the geometry of the molecule in its excited state. In general this rearrangement occurs very rapidly since it is governed by the speed of nuclear motion. Since the solvent cage and the molecule have

Figure II

Franck-Condon Jablonski Diagram

The Franck-Condon principle states that electronic motion is much faster than nuclear motion. Immediately after excitation, the molecule is in the Franck-Condon excited state, $S_1(\text{FC})$ and undergoes rapid vibrational relaxation. During the lifetime of S_1 , there is ample time for rapid solvent cage and molecular relaxation to accommodate the molecule in its excited state. This causes slight stabilization of S_1 to the equilibrium excited state, $S_1(\text{EQ})$, from which fluorescence may occur to $S_0(\text{FC})$, the Franck-Condon ground state. A molecule in $S_0(\text{FC})$ has the same molecular and solvent cage geometry as $S_1(\text{EQ})$ and thus rearrangement of the solvent cage may occur to a more stable geometry which causes slight stabilization to $S_0(\text{EQ})$, the equilibrium ground state.



rearranged to a more stable geometry, the S_1 energy is lowered slightly and it is from the equilibrium excited state, $S_1(EQ)$, that intersystem crossing and fluorescence occur. Emission occurs to the Franck-Condon ground state, $S_0(FC)$, which has the same solvent cage and molecular geometry as $S_1(EQ)$ after which vibrational relaxation occurs to the 0th vibrational level. Again the molecule and solvent cage rearrange to a more stable geometry resulting in the equilibrium ground state, $S_0(EQ)$, which is lower in energy than $S_0(FC)$.

Because S_1 lies below T_2 , intersystem crossing is a thermally assisted process. Most of the molecules are in the 0th vibrational level of S_1 but a certain fraction of these are in a vibrational level isoenergetic with the 0th vibrational level of T_2 . This fraction is given by the Boltzmann distribution. Therefore, we postulate an Arrhenius temperature dependence for k_{isc} . Equation 3 becomes

$$\phi_f(T) = k_f / (k_f + k_{isc}(T) + k_{ic})$$

which can be rearranged to yield equation 6.

$$\phi_f(T)^{-1} = 1 + k_{isc}(T)/k_f + k_{ic}/k_f \quad (6)$$

Because $k_{ic} \ll k_f$, the last term of equation 6 drops out. Assuming that $k_{isc}(T)$ can be expressed in terms of an Arrhenius dependence, equation 6 becomes equation 7 and finally equation 8.

$$\phi_f(T)^{-1} - 1 = k_{isc}(T)/k_f \quad (7)$$

$$\phi_f(T)^{-1} - 1 = k_{isc}(t)/k_f = A \exp(-E_a/RT) \quad (8)$$

The final rearrangement of equation 8 yields equation 9.

$$\log_e(\phi_f(T)^{-1} - 1) = \log_e A - E_a/RT \quad (9)$$

Thus if our two assumptions of negligible internal conversion and an Arrhenius dependence of k_{isc} are correct, a plot of $\log_e(\phi_f(T)^{-1} - 1)$ versus T^{-1} will yield a straight line of slope $-E_a/R$. A straight line will also result in the extremely unlikely case that k_{ic} shows the same temperature dependence as k_{isc} . An Arrhenius plot will therefore yield a straight line only if one process competes with fluorescence and as suggested above this process is very likely to be intersystem crossing, however, the Arrhenius plot by itself cannot determine which process it is. A departure from linearity may indicate that either a second process is competing with fluorescence to depopulate S_1 , that the activation energy (E_a) is changing because the S_1 - T_2 energy difference is varying with temperature, or that the assumption that k_{isc} can be fit to an Arrhenius expression is invalid.

The measurement of an activation energy implies that there is a minimum energy below which intersystem crossing will not occur. Below this energy the probability of transition to T_2 is zero and above it the probability is some finite and constant value. This energy is clearly at least equal to the energy difference between the 0th vibrational levels of S_1 and T_2 . Methyl-2-anthroate and methyl-9-anthroate have $3N - 6$ or 84 fundamental modes of vibration, where N is the number of atoms in the molecule. Many of these modes

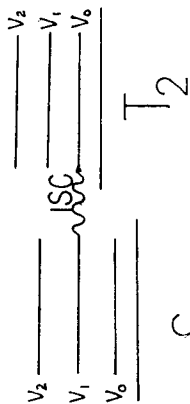
are low energy skeletal vibrations with the result that the density of vibrational states of S_1 at the 0th vibrational level of T_2 should be fairly high. Although not all of these vibrational modes are expected to have the proper symmetry to be involved in intersystem crossing, the probability that some of them will is probably high enough to assume that intersystem crossing occurs to the 0th vibrational level of T_2 . This assumption is further aided by the fact that in solution discrete vibrational levels are perturbed by the solvent environment. The effect of this is to smear the vibrational levels over a small but finite range of energies. If this assumption breaks down, however, then the activation energy obtained by the Arrhenius plot is not a measure of the T_2 energy but a measure of the barrier to intersystem crossing since the crossing would occur to some vibrational mode higher than the 0th vibrational level. In this case, the activation energy would be a poorer measure of the energy of T_2 relative to S_0 . Figure 3 shows the relationship between E_a as a measure of the triplet energy and the assumption that intersystem crossing occurs to the 0th vibrational level of T_2 ⁽⁸⁾. If the assumption holds, E_a is a good measure of the S_1 - T_2 energy gap, if not E_a is greater than the energy gap. Since E_a is a measure of the S_1 - T_2 gap, the sum of the S_1 energy and E_a should give a measure of T_2 relative to S_0 in both methyl-2-anthroate and methyl-9-anthroate. Since triplet states are fairly insensitive to solvent polarity, this sum might be much

Figure 3

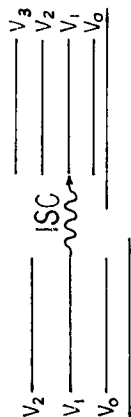
Relationship Between E_a and the
Singlet-Triplet Energy Gap

The activation energy, E_a , is a good measure of the singlet-triplet energy gap when intersystem crossing (ISC) occurs to the 0th vibrational level of T_2 , but E_a will be a poorer measure of the S_1 - T_2 energy gap when intersystem crossing occurs to higher vibrational levels.

↑ ENERGY



E_A A GOOD MEASURE
OF S_1-T_2 GAP



E_A A POOR MEASURE
OF S_1-T_2 GAP

less dependent on solvent polarity than either S_1 or E_a .

Previous interpretations of E_a relied on a classical crossing point explanation of the intersystem crossing process and the relationship between E_a and the singlet-triplet energy gap. Other data presented in this work suggests that the Franck-Condon factor or degree of vibrational overlap is at least a viable alternative interpretation.

EXPERIMENTAL

II. EXPERIMENTAL

Chemicals

Methyl-2-anthroate (2-COOMe) was prepared and purified by Matthews⁽⁹⁾ and used without further purification in this work. Methyl-9-anthroate (9-COOMe) previously prepared⁽¹³⁾ was found to be impure by observation of two shoulders at 380 and 400 nm superimposed upon the broad structureless emission spectrum of 9-COOMe in ethanol. It is speculated that the impurity was the anion of 9-anthroic acid which was produced from the decomposition of 9-COOMe. Therefore a new batch of 9-COOMe was synthesized⁽¹⁹⁾. Recrystallization of the crude product from hexane was found to be preferable to the recrystallization from ethanol which was suggested in the synthesis procedure⁽¹⁹⁾. A check on the purity consisted of a melting point determination (found 110.5-111.5°C, lit. 112°C⁽²⁰⁾) and the absence of the previously described impurity peaks.

Phenyl-9-anthroate was prepared and purified by Torrisi⁽²¹⁾ and used without further purification. Anthracene, obtained from Eastman Chemicals, and phenylethyl alcohol, obtained from Matheson, and Bell, were used without further purification. Benzyl-9-anthroate (9-COOMe) and phenylethyl-9-anthroate (9-COOMe) were synthesized by adapting a method⁽¹⁹⁾ described in the literature for the

esterification of hindered acids. In order to be certain that the reaction had gone to completion, the reactants in both syntheses were allowed to react for a week at room temperature. The low vapor pressure at room temperature of both alcohols used in the esterification of 9-anthroic acid necessitated vacuum distillation for their removal. The first attempt to isolate 9-COOPE resulted in its decomposition to anthracene as indicated by the NMR, absorption and fluorescence spectra of the decomposition product. Decomposition was attributed to the high temperature at which the vacuum distillation was conducted (130°C at 10 mm aspirator pressure). When a vacuum pump in conjunction with a liquid nitrogen trap was used, distillation occurred at 70°C and 1-2 mm pressure. Isolation of the desired product was considerably hastened by the addition of 5 ml of benzene. Benzene, which boils quite violently at 70°C and 1-2 mm pressure, caused spattering of the benzene-phenyl-ethyl alcohol solution of 9-COOPE against the walls of the container. Before the solution was able to drip down the sides, the solvent vaporized leaving the product adhered to the walls. The product was collected and washed with 10% NaOH. Recrystallization from ethanol was found to be preferable to recrystallization from hexane. 9-COOPE occurred as fluffy off-white flakes with a melting point of $91.5\text{--}92.5^{\circ}\text{C}$ and was characterized by NMR (singlet 8.2ppm, 1H; multiplet 7.6 ppm, 4H; multiplet 7.0 ppm, 9H; triplets 4.5 and 2.8 ppm

2H each, IR (carbonyl stretch at 1708 cm^{-1}) and fluorescence spectra (broad, structureless emission spectrum characteristic of 9-esters).

The 9-COOBe ester was isolated in a similar way. It occurred as bright yellow granular crystals with a melting point of $115\text{--}116^{\circ}\text{C}$ and was characterized by NMR (singlet 8.4 ppm, 1H; multiplet 7.9 ppm, 4H; multiplet 7.4 ppm, 9H; singlet 5.6 ppm, 2H) IR (carbonyl stretch at 1710 cm^{-1}) and by its characteristic fluorescence emission spectrum.

Solvents

All solvents were Matheson, Coleman and Bell Spectro-quality solvents except cumene (b.p. $151\text{--}153^{\circ}\text{C}$). A fluorescence check made on this solvent at the highest sensitivity of the MPF-2A showed negligible emission between 380 and 600 nm with an excitation wavelength of 360 nm. Therefore it was used without purification.

Instrumentation

Because all work was done on the Cary 118C and the MPF-2A, the monochromators of the two instruments were calibrated against each other as follows to insure reproducibility of results. The calibration is performed using a holmium oxide filter with an absorption spectrum accurately known⁽²²⁾ to .1 nm. A comparison of the known spectrum with the one obtained using the Cary 118C will yield a wavelength correction factor at various wavelengths which is usually small but does approach 1 nm near 450 nm.

Figure 4 shows the wavelength correction curve.

The calibration procedure for the excitation and emission monochromators in the MPF-2A instruction manual was followed except that the holmium oxide filter was used in place of the suggested neodymium oxide filter. The emission monochromator of the MPF-2A was calibrated against the Cary 118C by adjusting it so as to correctly record the position of the 360 nm holmium oxide absorbance. The excitation monochromator was then calibrated against the emission monochromator by reflecting the excitation beam through the emission monochromator which is set at 360 nm. It should be noted that the holmium oxide filter is not used in calibration of the excitation monochromator. Finally, the excitation monochromator was adjusted so that the excitation spectrum showed a peak at 360 nm. Although the wavelength corrections may seem trivial, a 1 nm error in the absorption measurement coupled with another 1 nm error in the same direction in the setting of the excitation monochromator wavelength can result in serious error in the determination of fluorescence quantum yields and activation energies. It has been shown that for 9-COOH an error of one nm in the excitation wavelength setting results in a 6% change in the quantum yield⁽²³⁾.

Determination of ϕ_f and E_a are described in detail by Hawkins⁽⁸⁾. The following changes are noted. Excitation wavelengths used in the temperature dependent studies of ϕ_f

TABLE I. WAVELENGTH CORRECTION FACTORS FOR CARY 118C

| <u>True Holmium Oxide</u> | <u>Holmium Oxide λ_{\max}</u> | |
|---|--|---------------------------------|
| <u>absorbance (λ_{\max}) (22),^a</u> | <u>from Cary 118C^a</u> | <u>Correction^{a,b}</u> |
| 279.3 | 279.0 | 0.3 |
| 287.6 | 287.2 | 0.4 |
| 333.8 | 333.2 | 0.6 |
| 360.8 | 360.2 | 0.6 |
| 385.8 | 384.6 | 0.8 |
| 418.5 | 417.8 | 0.7 |
| 446.0 | 444.9 | 1.1 |
| 453.4 | 452.3 | 1.1 |
| 536.4 | 535.3 | 1.1 |

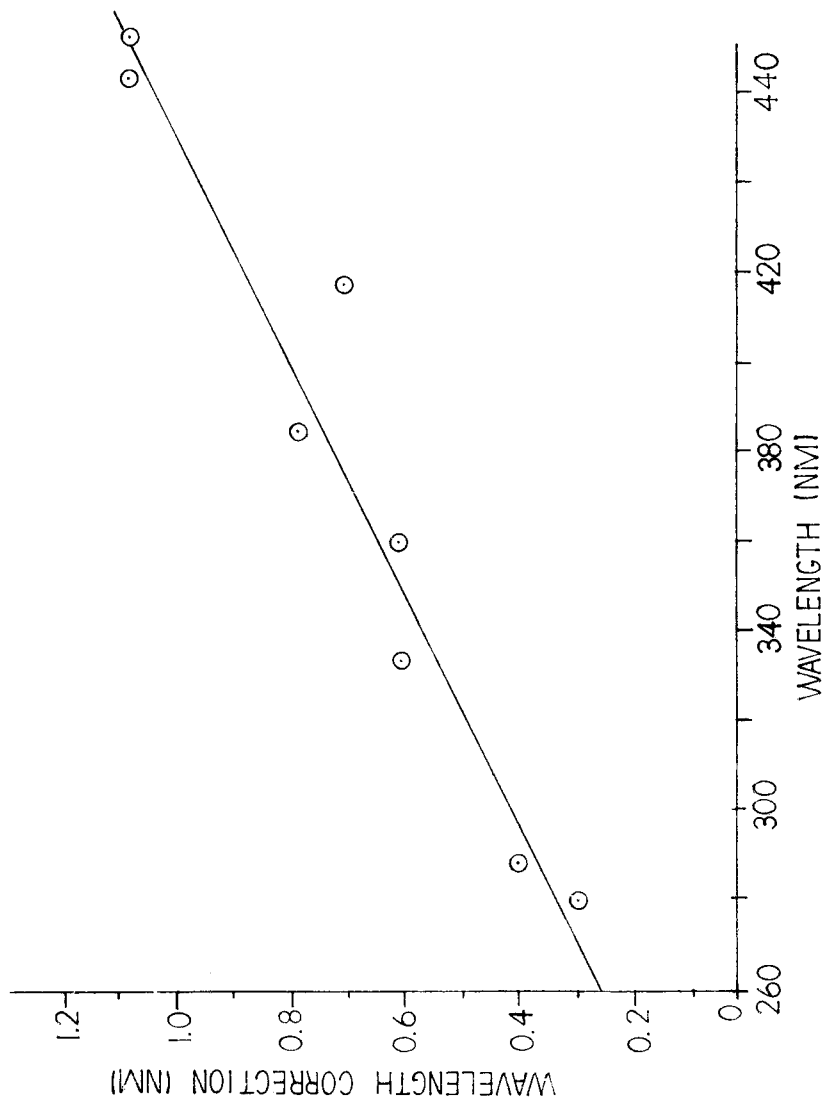
^a Units=nanometers

^b Add correction factor to Cary 118C absorbance to get true absorbance

Figure 4

Wavelength Correction Curve for Cary 118C

Wavelength correction factors for the Cary 118C are plotted as a function of the wavelength indicated on the instrument. These correction factors (in nm) are to be added to the wavelength indicated on the instrument to obtain the actual wavelength.



are chosen to correspond to valleys in the absorption spectrum; usually the valley between the 0-1 and 0-2 vibronic bands. The advantage of this is that absorbances corresponding to this wavelength are nearly insensitive to temperature and in many cases an absorption correction is not necessary since it is usually less than 1% over the whole temperature range and much less than other corrections applied.

The reference quantum yield, that of 9-COOme in ethanol, has been changed from .18 to .173 which is an average of .18⁽²⁴⁾ and .165⁽²⁵⁾, two values reported in the literature. Both values ultimately relied on quinine sulfate in 0.1 N H_2SO_4 as a reference quantum yield and hence it was not possible to decide between the two. In addition, it was not possible for us to improve upon or decide between the two using our techniques; hence we took an average as the quantum yield of our reference: 9-COOme in ethanol.

The procedure for measuring quantum yields has been improved as follows. Triplicate 5-10 ml samples of both the reference solution and solution whose quantum yield is to be measured (unknown) are made up such that the absorbance of each sample is less than 0.25 at the exciting wavelength. For each solvent used a solvent vs. solvent baseline is first run over the absorbance range of interest, usually 400-340 nm, recording pen period, scan speed and slit width. Once these are set they should not be changed during a

particular quantum yield determination. Before the baseline was run, the Cary 118C was zeroed at a wavelength at which the sample did not absorb (450 nm). The absorption spectrum for each sample of a given type was recorded over the solvent baseline. Before each sample was run, the Cary 118C was rezeroed at 450 nm.

The excitation wavelength cannot be chosen until after the absorption spectrum is recorded. In choosing the exciting wavelength, it has been found that the peak of the 0-1 vibronic band for both reference and unknown samples is nearly ideal in that the source radiation is of nearly equal intensity at these wavelengths. A rhodamine B quantum counter was used to obtain a lamp intensity vs. wavelength curve for the Xe lamp-excitation monochromator combination. This curve was used to obtain a lamp intensity correction factor which takes into account that the source intensity is not the same at the excitation wavelengths of the sample and unknown.

It was found that in order to obtain reproducible fluorescence quantum yield measurements, it was necessary to record the fluorescence spectra of reference and sample on the same sample sensitivity of the MPF-2A. Often it was necessary to dilute the samples whose quantum yields were to be determined to an absorbance of 0.07-0.09. Both reference and unknown samples were diluted by a factor of 10 and in all cases each sample had an absorbance of less than

0.025 at the exciting wavelength. It is recommended that all samples not be diluted by a factor other than 10 since this results in greater accuracy in sample dilution, ease of calculating results and conservation of solvent.

In recording the fluorescence spectrum of the diluted reference and unknown, a solvent background was recorded using the same excitation wavelength and sample sensitivity as for the sample. All samples of a given type were run on the same piece of chart. Calculations⁽²⁶⁾ have been performed in the literature that show that the 7 nm excitation slit and the 3 nm emission slit used in recording fluorescence spectra on the MPF-2A were small enough so that the $(n_u/n_r)^2$ correction factor used in our calculation of ϕ_f was applicable. For greatest reproducibility in recording fluorescence spectra, the MPF-2A was operated in the reference mode.

Other techniques which have been modified involve degassing and temperature measurement. Degassing can be hastened by performing the first cycle in the freeze-thaw degas cycle using only the rough pump pressure rather than the mercury diffusion pump. It is clear from the bubbling upon thawing that most of the degassing takes place under rough pump pressures. Finally, the Keithley digital voltmeter and copper-constantan thermocouple were calibrated together by measuring the voltage output of the thermocouple in an ethanol temperature control bath over the temperature

range from 10-76°C. The temperature of the bath was monitored with a thermometer capable of reading to 0.02°C, and the bath unit was the same as that used in the temperature dependent studies of ϕ_x . Frequent recalibration of the thermocouple-voltmeter combination should be done. Figure 5 shows the voltmeter-thermocouple correction curve.

An additional area of work involved the suspending of anthracene, 2-COOMe and 9-COOMe in polymethylmethacrylate (PMM). Methylmethacrylate was obtained from Matheson, Coleman and Bell in two grades, reagent grade (b.p. 100-101°C) and Chromoquality (99+ mole per cent), but only the reagent grade which was stored at 0°C was used. After dissolving one of the above compounds in the monomer such that the absorbance of the solution was about 1.0 in a 1 cm cell the solution was placed in 8 mm glass tubing, degassed and sealed under vacuum. The sealed tubing was placed in a circulating temperature-controlled silicone oil bath at temperatures between 75 and 85°C as shown in Figure 6. The tubing was held in place by hooking one end of a paper clip in a piece of tape attached to the top of the tubing and hooking the other end to the edge of the bath container. A heating rod was used to bring the bath to the desired temperature and a Variac potentiometer control was used to keep the temperature within $\pm 0.5^\circ\text{C}$ of this value. After a week of heating, initial attempts at polymerization did not succeed but resulted in very viscous, somewhat rubbery solutions. Attempts to polymerize the monomer itself resulted in the same

Figure 5

Thermocouple-Voltmeter Temperature Correction Curve

Temperature measurements were made using a copper-constantan thermocouple with the reference junction at 0°C and a Keithley digital voltmeter. A plot of the millivolt readout of the copper-constantan-voltmeter combination versus temperature (degrees Celsius) is given on the next page and was used in the calculation of temperature in the temperature control block of the MPP-2A in measurements of E_a .

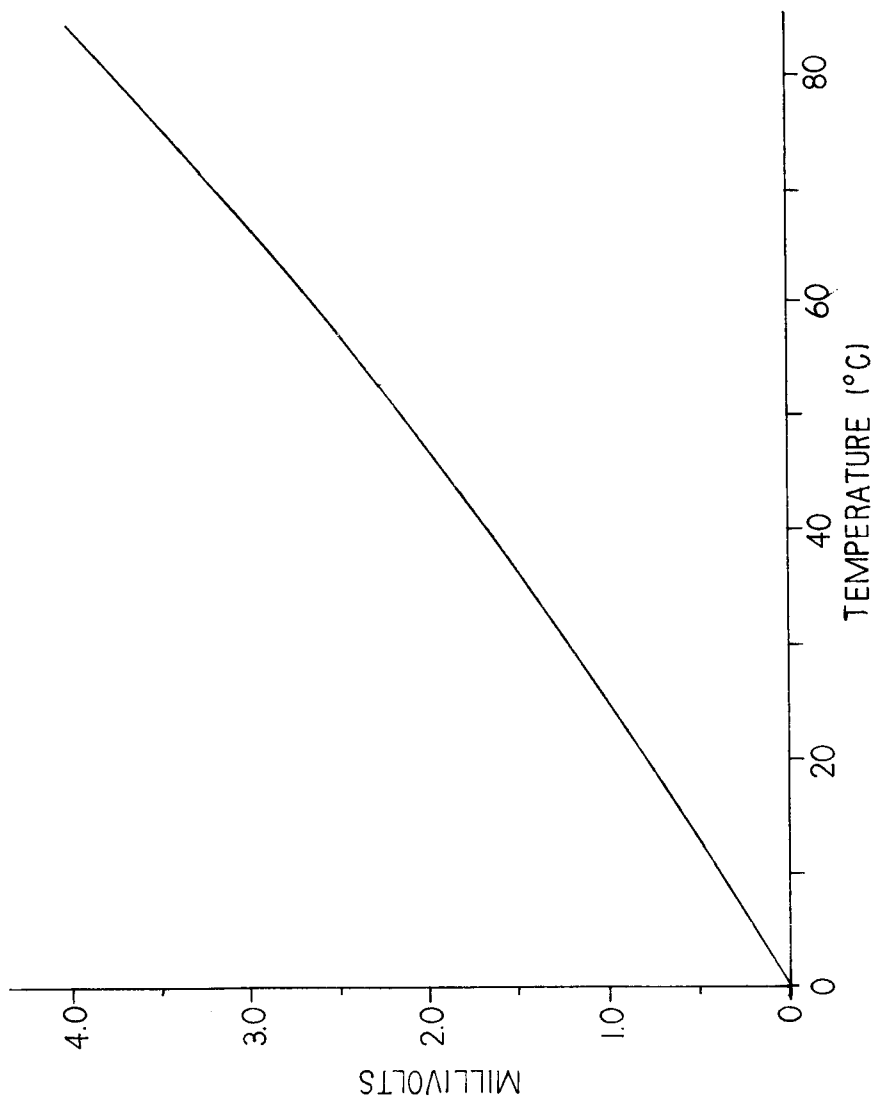
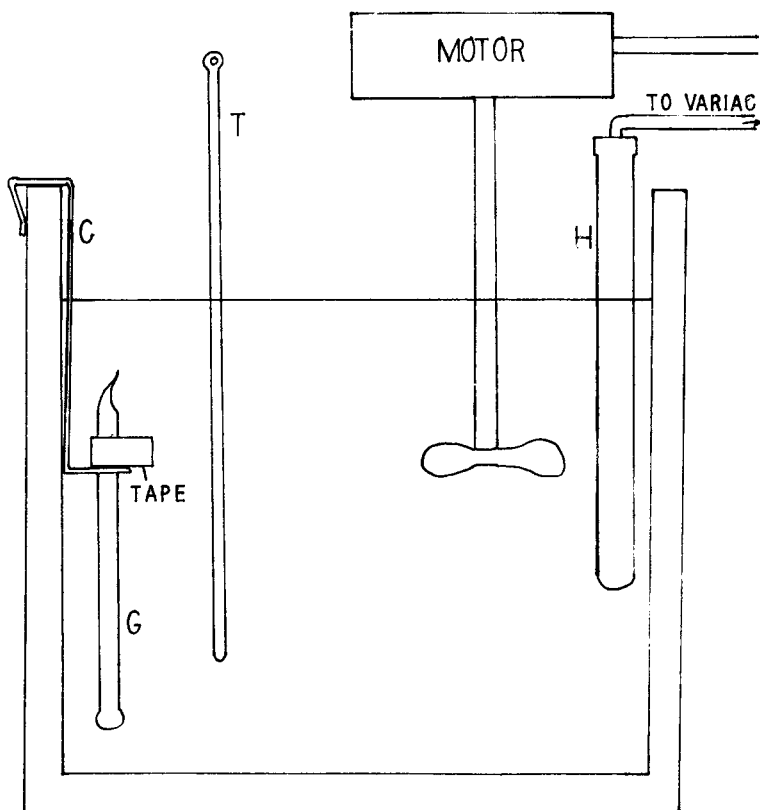


Figure 6Temperature Controlled Silicone Oil Bath Used In
Polymerization of Methyl Methacrylate

A heating rod (H) is used to heat a silicone oil bath to about 80°C. The temperature is checked with a thermometer (T) and a motor is used to drive a propellor which ensures even temperature distribution. A piece of tape is wrapped around the upper portion of a piece of glass tubing (G) and inserted through a loop in the end of a piece of copper wire (C) which rests on the edge of the bath. The entire glass tubing is submerged to allow an even temperature distribution within the tube.



rubbery medium. Addition of azo-bis(isobutyronitrile) as a catalyst in concentrations of 10 ppm caused polymerization to occur more completely but the resulting rod of PM was quite flexible although hardening on exposure to air did occur. However, it has been shown that this catalyst can quench phosphorescence and thus we will want to avoid its use when measurements are made. Presumably polymerization was inhibited by such impurities as methacrylic acid from condensation from repeated exposure of the cold solvent to the atmosphere. Therefore the solvent was purified⁽²⁷⁾ as described in the literature except that a silica-gel column was not used. The purified methylmethacrylate was stored under dry nitrogen and refrigerated. The above solutions were then prepared with the purified monomer and heated as described previously. Complete polymerization occurred within two days. The rod of PM which resulted was clear, hard, not rubbery and had the appearance of a glass rod.

RESULTS

III. RESULTS

Table II gives a summary of absorption, fluorescence emission, and fluorescence quantum yield data for the compounds studied in the solvents indicated. Since the absorption spectra for all the compounds in the table show a high degree of vibrational structure, the energy in Table II corresponds to λ_{\max} for the 0-0 absorption band. These values are relatively unaffected by solvent polarity. In the case of methyl-9-anthroate, the absorption energies show a variation of about 360 cm^{-1} , while methyl-2-anthroate shows a variation of 310 cm^{-1} over the solvent polarity range. Little correlation can be made between 0-0 energies and solvent polarity other than the values in aromatic solvents are the most red-shifted. The fluorescence emission energies are a measure of the equilibrium excited state relative to the Franck-Condon ground state. Since excitation in 9-COOMe is accompanied by a large change in molecular geometry, its emission spectrum is broad and structureless in all solvents except cyclohexane where slight structure does appear. Apparently the presence of bulky ester groups such as *p*-nitrophenyl, benzyl and β -phenylethyl have no effect on excited state rotation of the carboxyl group since the emission spectra for all of the 9-carboxylic acid esters are broad and structureless. Because of this the S_1 energies for the 9-derivatives listed in Table II are just λ_{\max} for the corrected emission spectrum. Methyl-2-anthroate exhibits a structured emission spectrum in

TABLE II

Absorption and Fluorescence Energies, Fluorescence Quantum Yields for Esters of 2- and 9-Anthroic Acid in Solvents for the $E_T(30)$ Values Listed. Fluorescence Energies are λ_{\max} for 9-COOMe and O-O Energies for 2-COOMe.

| Compound | Solvent | Absorption (cm^{-1}) | Fluorescence (cm^{-1}) | $\phi_f(22^\circ\text{C})$ | $E_T(30)$ |
|--------------------------------------|-------------------|------------------------------------|--------------------------------------|----------------------------|-----------|
| Methyl-9-anthroate | | | | | |
| | Methanol | 26,350 | 20,964 \pm 89 | .083 \pm .003 | 55.5 |
| | Ethanol | 26,322 | 21,053 \pm 89 | .173 \pm .008 | 52 |
| | Acetonitrile | 26,302 | 21,413 \pm 91 | .38 \pm .02 | 46 |
| | Benzonitrile | 25,990 | 21,322 \pm 91 | .75 \pm .03 | 42 |
| | Toluene | 26,123 | 21,834 \pm 96 | .78 \pm .03 | 33.9 |
| | Benzene | 26,123 | 21,834 \pm 96 | .82 \pm .03 | 34 |
| | Cyclohexane | 26,302 | 22,222 \pm 50 | .76 \pm .03 | 33 |
| | p-Dioxane | 26,191 | 21,786 \pm 92 | .85 \pm .03 | 36 |
| Methyl-2-anthroate | | | | | |
| | Benzonitrile | 25,138 | 23,964 \pm 14 | .90 \pm .04 | 42 |
| | Benzene | 25,227 | 24,486 \pm 14 | .80 \pm .03 | 34 |
| | Toluene | 25,240 | 24,510 \pm 14 | .72 \pm .03 | 33.9 |
| | Cumene | 25,264 | 24,582 \pm 14 | .68 \pm .03 | 33.5 |
| | Acetonitrile | 25,450 (a) | 24,150 \pm 14 (a) | .92 \pm .04 (a) | 46 |
| | Ethanol | 25,380 (a) | 23,500 \pm 14 (a) | .90 \pm .04 | 52 |
| | Trifluoro-ethanol | 25,380 (a) | 22,000 \pm 100 (a) | .88 \pm .04 | 61.1 |
| | p-Dioxane | 25,350 (a) | 24,600 \pm 14 (a) | .83 \pm .03 (a) | 36 |
| | Cyclohexane | 25,380 (a) | 25,000 \pm 14 (a) | .47 \pm .02 (a) | 33 |
| | Hexane | 25,410 (a) | 25,200 \pm 14 (a) | .32 \pm .01 (a) | 30 |
| 9-(p-nitrophenyl)-anthroate | | | | | |
| | Cyclohexane | 26,212 | | .14 \pm .01 (b) | 33 |
| 10-Bromo-9-(p-nitrophenyl)-anthroate | | | | | |
| | Cyclohexane | 26,042 | | .19 \pm .01 (b) | 33 |
| (p-phenylethyl)-9-anthroate | | | | | |
| | Cyclohexane | 26,290 | | | 33 |
| Benzyl-9-anthroate | | | | | |
| | Cyclohexane | 26,288 | | | 33 |

^aSee Reference 8

^bSee Reference 21

all solvents except 2,2,2-trifluoroethanol so the energies for 2-COOMe given in Table II are O-O band energies. The S_1 energies for 9- and 2-COOMe are relatively sensitive to solvent polarity showing a red shift with increasing solvent polarity and polarizability. In aromatic solvents, the red shift may be due to weak π - π interactions between solute and solvent.

The fluorescence quantum yields in this work are based on a reference quantum yield (9-COOMe in ethanol) of 0.173 rather than on the previous value of 0.18. Therefore, previous ϕ_f values⁽⁸⁾ have been adjusted to compensate for the change by multiplying the old value by a factor of 0.173/0.18. Our ϕ_f values for 2-COOMe in benzene, trifluoroethanol and ethanol do not agree well with the previous work⁽⁸⁾ even after the adjustment has been made for the change in reference quantum yield. A comparison of the degassing factors and refractive index correction factors with the previous work shows good agreement, hence the discrepancy must lie in the fact that we performed all ϕ_f determinations on the same sample sensitivity setting of the MPF-2A while those of Hawkins were done on different sample sensitivities. We believe that our method is an improvement since the quantum yields for 2-COOMe in benzene could not be determined reproducibly when measurements were made using different sample sensitivities. Once the measurements were made using the same sample sensitivity settings, the precision for each quantum yield was on the order

of one percent. Even measurements taken by different workers agreed to within one percent of each other when using the newer method. Details of the calculation of ϕ_f are presented elsewhere(8).

Table III gives a summary of activation energies and fluorescence lifetimes for the compounds studied in various polar, non-polar and aromatic solvents. The fluorescence quantum yields of each compound in these solvents were determined as a function of temperature and were fit to an Arrhenius plot as described earlier. The slope of the line thus obtained is multiplied by $-1.987 \text{ cal mole}^{-1} \text{ deg}^{-1}$ to yield the activation energy in cal mole^{-1} which is then converted to an energy in kcal mole^{-1} . Although not shown, the correlation coefficient for the 95% confidence interval for almost each Arrhenius fit was generally better than 0.98 indicating good linearity.

Error limits for the activation energy arise from the uncertainty of about 5% in our reference quantum yield. Hence all the room temperature quantum yields measured in this work are accurate to $\pm 5\%$. For each solvent, then, an upper and lower limit for the activation is calculated by using the corresponding upper and lower limits on the room temperature quantum yield in the calculation of E_a .

As Table III indicates a 5% error in ϕ_f does not always result in a 5% error in E_a . For low ϕ_f 's (~ 0.25), the error in E_a is about 1%; for intermediate ϕ_f values ($0.25-0.65$), the error is approximately 5-10% and for high ϕ_f values ($0.7-0.85$),

TABLE III

Fluorescence Lifetimes and Activation Energies for 2-COOMe and 9-COOMe in Solvents for the $E_T(30)$ Solvent Polarity Values Listed

| Compound | Solvent | τ_f (nsec) ^{b,c,d} | E_a (kcal/mole) | $E_T(30)$ |
|--------------------------------------|-------------------|----------------------------------|-------------------------------|-----------|
| Methyl-9-anthroate | | | | |
| | Methanol | 1.7 \pm 1 | 3.97 \pm .02 | 55.5 |
| | Ethanol | 4.1 \pm .6 | 4.35 \pm .05 | 52 |
| | Acetonitrile | 8.1 \pm .5 | 3.45 \pm .15 | 46 |
| | Benzonitrile | 12.7 \pm .5 | 2.66 \pm .39 | 42 |
| | Toluene | | 2.66 \pm .33 | 33.9 |
| | Benzene | 14.1 \pm .5 | 3.58 \pm .57 | 34 |
| | Cyclohexane | 12.5 \pm 1 | 2.25 \pm .35 | 33 |
| | p-Dioxane | 14.4 \pm .5 | 6.39 \pm 1.12 | 36 |
| Methyl-2-anthroate | | | | |
| | Benzonitrile | 19.2 \pm .2 | 2.5 \pm 1.0 | 42 |
| | Benzene | 17.7 \pm .1 | 3.25 \pm .50 | 34 |
| | Toluene | 16.0 \pm .2 | 2.40 \pm .20 | 33.9 |
| | Cumene | 15.3 \pm .2 | 2.28 \pm .30 | 33.5 |
| | Acetonitrile | 21.5 \pm .5 | 3.5 \pm 1.0 | 46 |
| | Ethanol | 21.8 \pm .3 | 2.5 \pm 1.0 | 52 |
| | Trifluoro-ethanol | 27.2 \pm .5 | TIF* | 61.1 |
| | p-Dioxane | 19.1 \pm .2 | 3.48 \pm .53 ^(a) | 36 |
| | Cyclohexane | 10.3 \pm .2 | 2.45 \pm .15 ^(a) | 33 |
| | Hexane | 9.8 \pm .2 | 1.87 \pm .10 ^(a) | 30 |
| 9-(p-nitrophenyl)-anthroate | | | | |
| | Cyclohexane | 2.4 \pm .5 | 2.33 \pm .02 | 33 |
| 10-Bromo-9-(p-nitrophenyl)-anthroate | | | | |
| | Cyclohexane | 3.0 \pm .5 | 2.9 \pm .03 | 33 |

*Temperature Independent Fluorescence

^aSee Reference 8

^bValues for 9-COOMe were determined by Dr. Bunting at Tufts

^cValues for 2-COOMe were determined by Dr. Iytle at Purdue

^dValue for 9-COOMe in ethanol was determined by Dr. T. C. Werner at MIT (Ph.D. thesis)

the error is about 10-30%. In the case that ϕ_f is greater than about 0.85, the error is on the order of 50% and this method becomes unreliable because the change in fluorescence intensity with increasing temperature for a molecule in a given solvent becomes exceedingly small at high ϕ_f values and approaches the magnitude of the refractive index and absorption correction factors applied. Alternatively, the change in k_{isc} with increasing temperature is too small when compared with the magnitude of k_f to accurately measure E_a . Therefore little can be said about the activation energy for 2-COOMe in benzonitrile and ethanol where $\phi_f=0.90$ except that the activation energy must be high because the fluorescence intensity is nearly temperature independent in these solvents.

Arrhenius plots for 9-COOMe in benzene and toluene show slight curvature while those for 9-COOMe and 2-COOMe in benzonitrile show gross deviation from linearity as shown in Figure 7. It was found that in the latter case that fluorescence energies blueshifted by approximately 200 cm^{-1} with increasing temperature over a 90° range. The curvature of the Arrhenius plots in aromatic solvents increases with increasing temperature and is probably a reflection of the fact that S_1 is blueshifting much less rapidly with temperature than E_2 so that the activation energy must be correspondingly higher. Another possibility, although less likely, is internal conversion at high temperatures. This effect may be viewed as a breaking

Figure 7a

ϕ_f vs Temperature for 9-COOMe in
Benzene, Toluene and Benzonitrile

Arrhenius plots for 9-COOMe in benzene, toluene and benzonitrile show deviation from linearity. Since the slope of the plot is proportional to the activation energy, the curvature of these plots indicates that S_1 is dropping relative to T_2 with increasing temperature rather than a reflection of the occurrence of internal conversion.

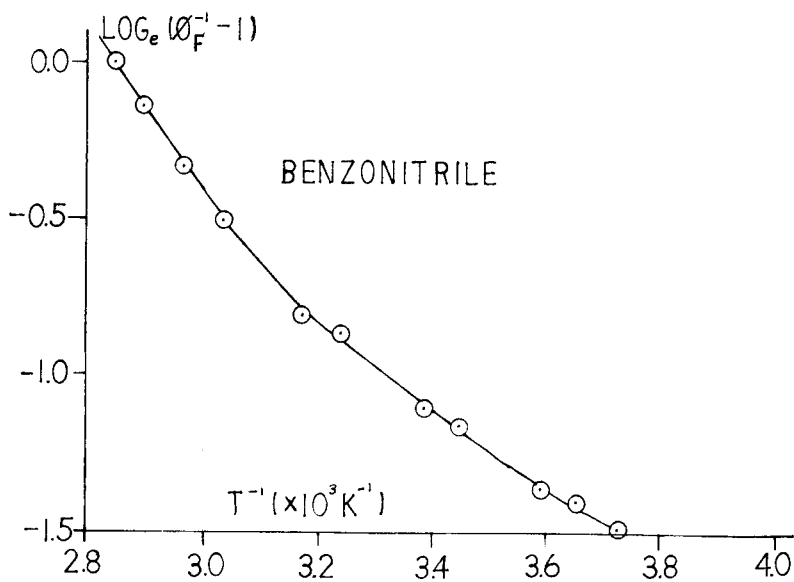
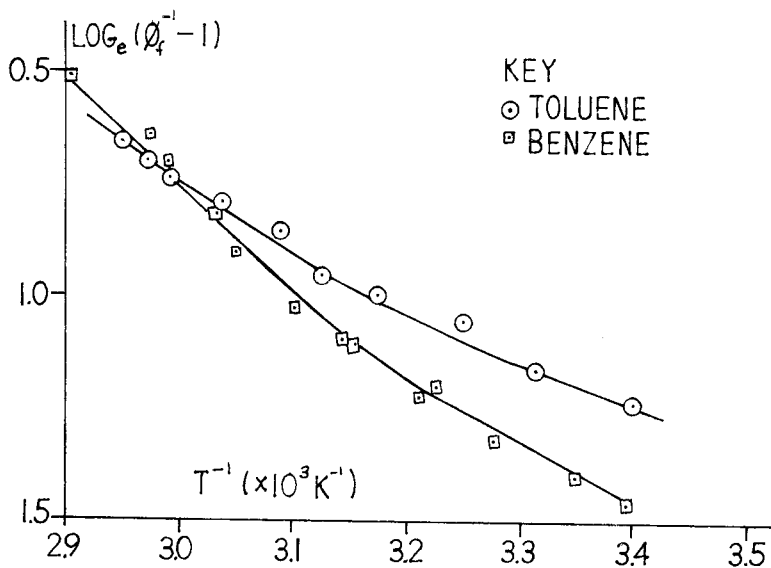
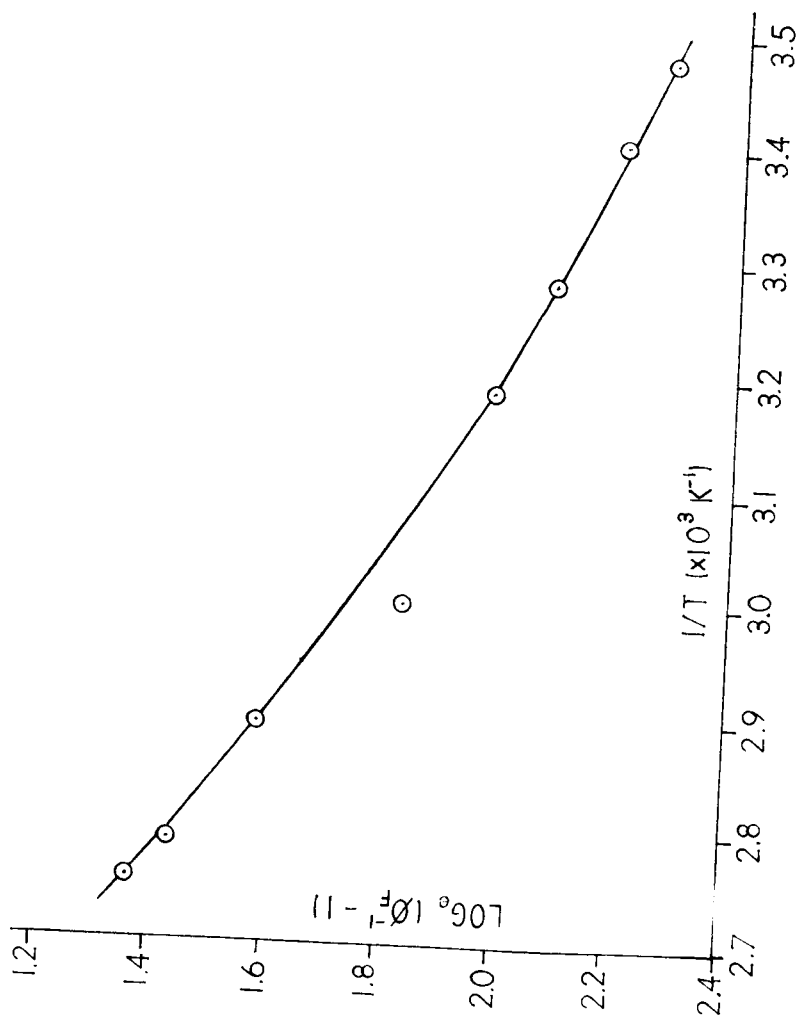


Figure 7b

ϕ_f vs Temperature for 2-COOMe in Benzonitrile

The Arrhenius plot for 2-COOMe in benzonitrile shows deviation from linearity which is also probably an indication of an increasing S_1-T_2 energy gap with increasing temperature.



of the solute-solvent π - π interactions with increasing temperature. These interactions are observed generally in other aromatic solvents. The S_1 energies have been observed to red-shift in solvents such as mesitylene, 1,2,3-trimethylbenzene, p-xylene, tert-butyl-benzene and even pyridine indicating the importance of these weak π - π solute-solvent interactions.

DISCUSSION

IV. DISCUSSION

The singlet and triplet energy levels of anthracene can be used as a point of departure in describing the energy levels of 9-COOMe and 2-COOMe. It has been fairly well established that the S_1 energy level in anthracene lies slightly above a nearby triplet, probably T_2 . The fluorescence spectrum of anthracene gives an S_1 energy of $26,700 \text{ cm}^{-1}$ (8,12). The phosphorescence spectrum indicates that the lowest triplet (T_1) lies at $14,700 \text{ cm}^{-1}$ and triplet-triplet absorption studies indicate that T_2 lies at $26,050 \text{ cm}^{-1}$ (12). Substitution on the parent compound reduces its symmetry and lowers the S_1 energy relative to the ground state (S_0). The triplet manifold in anthracene seems to be nearly insensitive to substitution⁽¹²⁾ and less sensitive to solvent polarity than S_1 . The first excited singlet and T_1 and T_2 are $\pi\pi^*$ excited states. Studies of aromatic compounds⁽²⁸⁾ with acidic functional groups show that the pK_a 's of triplet states are very similar to the pK_a 's of molecules in the ground state, while the pK_a 's of excited singlet states are significantly different from ground state pK_a 's. This would indicate a similar electron distribution in the triplet manifold as in the ground state. Presumably this is also the case for 2-COOMe and 9-COOMe and hence may explain the relative independence of T_2 to substitution.

If S_1 lies above T_2 , as is the case with anthracene, intersystem crossing need not be thermally assisted. Crossing

from the 0th vibrational level of S_1 would occur to an iso-energetic vibrational level of T_2 with probability of transition dependent upon the Franck-Condon factor at this energy. Because k_{isc} is not dependent upon temperature, it is expected that ϕ_f will be independent of temperature. This is found to be the case for anthracene⁽⁸⁾. However, as described previously, when S_1 lies slightly below T_2 , k_{isc} may be dependent on temperature and hence ϕ_f will also be a function of temperature. Methyl-9-anthroate shows a decreasing quantum yield with increasing temperature in a variety of solvents of widely varying polarity indicating that S_1 is below T_2 . Methyl-2-anthroate shows a similar change in ϕ_f with temperature for all the solvents used in this work except for 2,2,2-trifluoroethanol, a highly polar hydrogen bonding solvent, indicating that S_1 is still below T_2 but that in trifluoroethanol, the S_1 level of 2-COOMe is too far below T_2 to allow for any appreciable temperature-dependent intersystem crossing. The quantum yield for 2-COOMe in trifluoroethanol at room temperature is 0.88 ± 0.03 which suggests that 12% of the molecules are being depopulated from S_1 by a non-radiative pathway, either internal conversion or temperature independent intersystem crossing. It does not seem likely that internal conversion to S_0 is important because of the mass of evidence resulting from deuteration studies performed on a wide variety of polynuclear aromatic hydrocarbons. Assuming that the T_1 energy in 2-COOMe and 9-COOMe is about the same as that in anthracene, the S_1-T_1

energy gap for 2-GOOMe in trifluoroethanol is about $7,500 \text{ cm}^{-1}$. Studies⁽³⁾ have been performed on the rate of triplet decay ($T_1 \rightarrow S_0$). It was assumed that the rate of radiationless inter-system crossing ($T_1 \rightarrow S_0$) is about equal to the rate of triplet decay. The rate constant for the process $T_1 \rightarrow S_0$ was estimated as a function of the T_1-S_0 energy gap. When the data was extrapolated to a zero energy gap, it was found that the rate constant for the radiationless process was $10^7-10^8 \text{ sec}^{-1}$ which is the rate constant for intersystem crossing ($S_1 \rightarrow T_2$) when S_1 and T_2 are close in energy. Hence, there may be some basis for assuming that these studies may be useful in estimating a k_{isc} when the singlet and accepting triplet are separated by considerable energies. Assuming that the S_1-T_1 energy gap of 2-GOOMe in trifluoroethanol is about 7500 cm^{-1} , then k_{isc} ($S_1 \rightarrow T_1$) is approximately 10^5 sec^{-1} , which is two orders of magnitude less than k_f in this solvent. Our calculations show that k_{isc} is actually on the order of 10^6 sec^{-1} which is not bad agreement. Other calculations of k_{isc} for 2-GOOMe in ethanol ($\phi_f=0.90$) using equation 11 which is developed later show that over the temperature range of $20-75^\circ\text{C}$, k_{isc} increases by $4 \times 10^6 \text{ sec}^{-1}$. Assuming that k_{isc} would show a similar increase for 2-GOOMe in trifluoroethanol, a change in ϕ_f can be calculated using equation 3. Such calculations show that ϕ_f would decrease from 0.38 at room temperature to 0.81-0.82 at 70°C , or about an 8% change. Since our methods would have been able to detect such a change in ϕ_f for 2-GOOMe in trifluoro-

ethanol, we can only deduce that the temperature independent fluorescence is a result of a temperature independent intersystem crossing (TIX) to T_1 . If any intersystem crossing occurs to T_2 it must be negligible. Presumably the enhanced intersystem crossing to T_1 is a result of the fact that the S_1 - T_1 energy gap is becoming smaller with increasing solvent polarity and that the probability of transition between states of different multiplicities depends inversely on the third power of the energy gap. Additional evidence for the magnitude of k_{isc} to T_1 comes from work done by Huber et al.⁽²⁹⁾. Huber has found that for 9,10-diphenylanthracene in cyclohexane ϕ_f , τ_f , and k_f are 0.95, 7.58 nsec, and $1.25 \times 10^8 \text{ sec}^{-1}$, respectively. A value of $6.6 \times 10^6 \text{ sec}^{-1}$ was calculated for k_{isc} . This molecule also shows temperature independent fluorescence and has a similar energy level scheme to that of 2-COOMe in trifluoroethanol, namely too large an S_1 - T_2 energy gap for temperature dependent intersystem crossing to be important and an S_1 - T_1 energy gap similar to that of 2-COOMe in trifluoroethanol. It is interesting that his value for k_{isc} to (presumably) T_1 is remarkably close to ours.

Table IV gives a summary of fluorescence lifetime data for 2-COOMe and 9-COOMe in various solvents and k_f for these molecules in the same solvents. The fluorescence rate constant was calculated from the quantum yields given in Table II and τ_f using equation 3. Figure 8 shows that k_f is fairly independent of solvent polarity for 2-COOMe and 9-COOMe. The

TABLE IV

Fluorescence lifetimes and activation energies for 2-COOMe and 9-JOOMe in polar, non-polar and aromatic solvents.

Fluorescence rate constants are calculated from ϕ_f and T_f .

| <u>Compound</u> | <u>Solvent</u> | <u>T_f(nsec)</u> | <u>$k_f(10^7 \text{sec}^{-1})$</u> | <u>$E_a(\text{cm}^{-1})$</u> |
|--------------------|-------------------|-------------------------------|---|---|
| Methyl-9-anthroate | | | | |
| | Methanol | 1.7 \pm 1 | 4.8 \pm 2.8 | 1374 \pm 110 |
| | Ethanol | 4.1 \pm 0.6 | 4.2 \pm 0.6 | 1520 \pm 20 |
| | Acetonitrile | 8.1 \pm 0.5 | 4.7 \pm 0.5 | 1210 \pm 50 |
| | Benzonitrile | 12.7 \pm 0.5 | 5.9 \pm 0.2 | 930 \pm 140 |
| | Toluene | | | 930 \pm 120 |
| | Benzene | 14.1 \pm 0.5 | 5.8 \pm 0.2 | 1250 \pm 200 |
| | Cyclohexane | 12.5 \pm 1 | 6.1 \pm 0.5 | 790 \pm 120 |
| | p-Dioxane | 14.4 \pm 0.5 | 5.9 \pm 0.2 | 2240 \pm 390 |
| Methyl-2-anthroate | | | | |
| | Benzonitrile | 19.2 \pm 0.5 | 4.7 \pm .3 | 870 \pm 350 |
| | Benzene | 17.7 \pm 0.2 | 4.5 \pm 0.3 | 1140 \pm 170 |
| | Toluene | 16.0 \pm 0.5 | 4.5 \pm 0.3 | 840 \pm 70 |
| | Cumene | 15.3 \pm 0.5 | 4.4 \pm 0.3 | 800 \pm 105 |
| | Acetonitrile | 21.5 \pm 0.5 | 4.3 \pm 0.3 | 1230 \pm 350 |
| | Ethanol | 21.8 \pm 0.3 | 4.1 \pm 0.3 | 870 \pm 350 |
| | Trifluoro ethanol | 27.2 \pm 0.5 | 3.2 \pm 0.2 | TIF* |
| | p-Dioxane | 19.1 \pm 0.2 | 4.3 \pm 0.2 | 1220 \pm 190 |
| | Cyclohexane | 10.3 \pm 0.2 | 4.6 \pm 0.2 | 880 \pm 50 |
| | Hexane | 9.8 \pm 0.2 | 3.3 \pm 0.2 | 650 \pm 35 |

*Temperature Independent Fluorescence

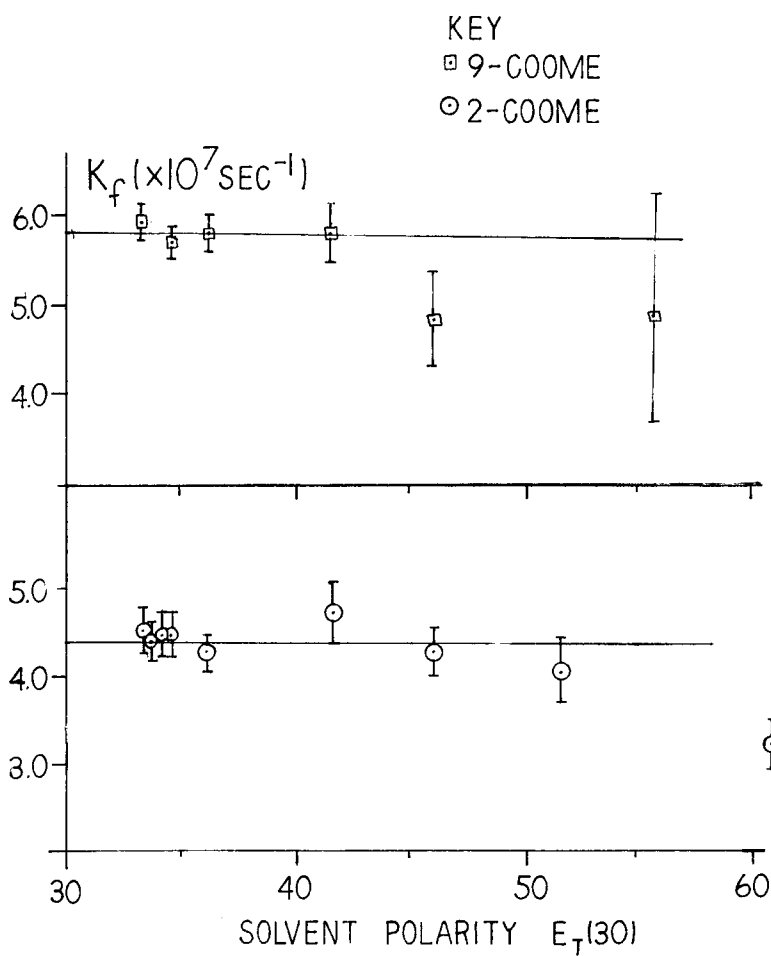
UN82 FACCI, J.S. THE EFFECT OF SOLVENT POLARITY, etc.
F137e/1977 Chemistry HRS. 4/77 2 of 2



Figure 8

Fluorescence Rate Constants for 9-COOMe and 2-COOMe
As a Function of Solvent Polarity

The fluorescence rate constants for 9-COOMe and 2-COOMe are fairly independent of solvent polarity for a given molecule indicating that k_f is a molecular property not dependent on effects of molecular environment. Deviation from the average k_f in 9-COOMe is probably due to the difficulty in measuring short lifetimes. Little deviation is noted for 2-COOMe in all solvents but 2,2,2-trifluorethanol.



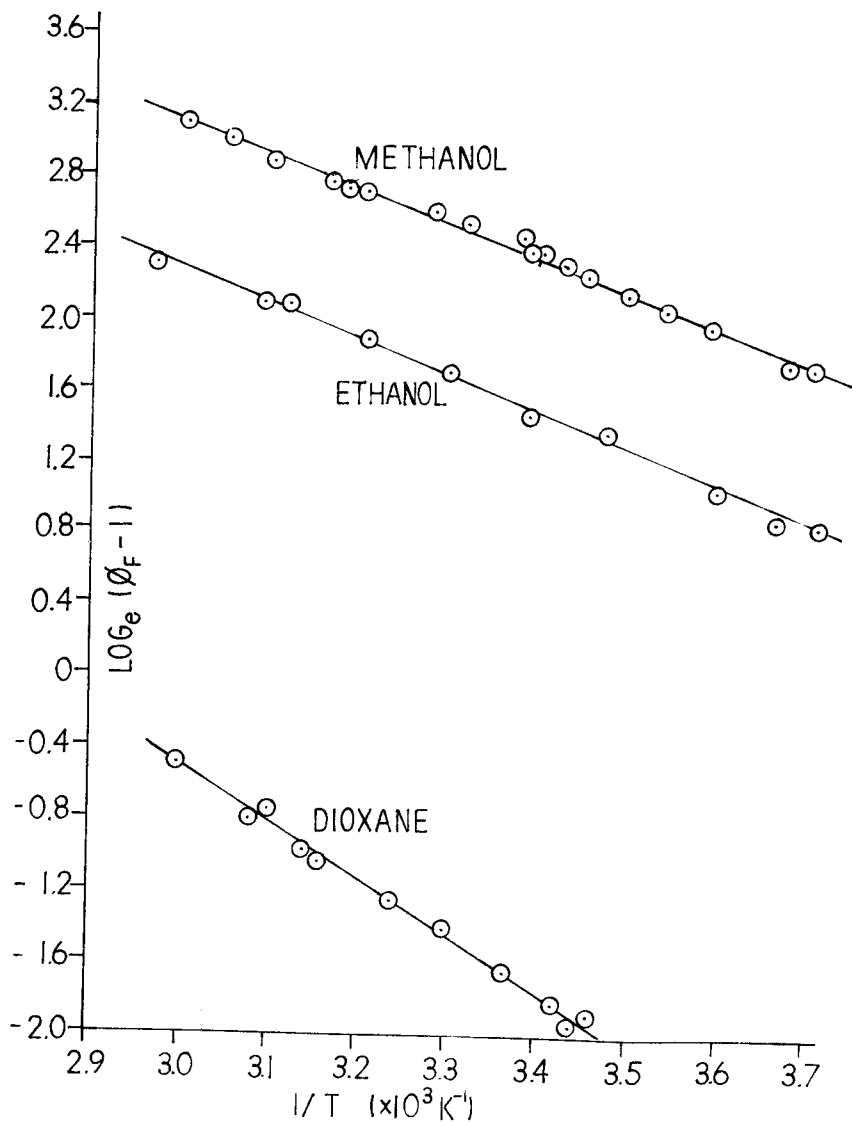
k_f value for 2-COOMe in trifluoroethanol is markedly lower than that for 2-COOMe in the other solvents due to an unusually long fluorescence lifetime. This measurement has been repeated several times and is a reliable one; ϕ_f for 2-COOMe in trifluoroethanol has also been repeated several times by two workers with an unusual degree of precision. Hence the k_f value for 2-COOMe in this solvent is probably correct. The deviation of k_f for 9-COOMe in ethanol and acetonitrile from the average value given by 9-COOMe in the solvents where k_f were approximately the same can be attributed to the difficulty in measuring short fluorescence lifetimes. Hence our original assumption that k_f is a molecular property not dependent on solvent effects has been shown to be correct. This would indicate that k_f is truly a first order rate process. Thomaz⁽⁴⁾ has suggested that the independence of k_f on environmental effects is due to equal fluorescence rate constant contributions from each of the vibrational levels of S_1 .

Assuming that internal conversion is negligible compared with k_f and k_{isc} , an activation energy (E_a) for the S_1 - T_2 energy gap can be calculated if k_{isc} is a thermally assisted process. Table IV gives a summary of E_a values for 9-COOMe and 2-COOMe in the solvents indicated. The E_a values are picked from the slope of an Arrhenius plot of $\log_e(\phi_f(T)^{-1} - 1)$ versus T^{-1} as described previously. This slope is multiplied by $-1.987 \text{ cal mole}^{-1} \text{ deg}^{-1}$ to obtain an

activation energy in cal mole⁻¹ which may then be converted to an energy in cm⁻¹. In general, the Arrhenius plots for 9-COOMe in non-aromatic solvents show a high degree of linearity as do those for 2-COOMe in non-aromatic solvents. In addition, these plots for 2-COOMe in all aromatic solvents but benzonitrile show good linearity. Figure 9 shows some of the Arrhenius plots for 9-COOMe in representative non-aromatic solvents. This linearity lends support to our hypothesis that intersystem crossing is the only temperature dependent process depopulating S₁. It has been suggested⁽⁴⁾ that the temperature dependence of k_{isc} in a given solvent is not due to changes in either the density of states or the Franck-Condon factor but to a change in the population of a vibrational level isoenergetic with the 0th vibrational level of T₂. Thomaz has pointed out that the population and depopulation of a vibrational level within an electronic state occurs much faster than the intersystem crossing process. It is important to note that Thomaz breaks the intersystem crossing process into two steps: the first is an equilibrium which exists between molecules in the 0th vibrational level of S₁ and molecules in a vibrational level isoenergetic with the 0th vibrational of T₂, the second is the transition from the singlet state to the triplet state, a process which results in no change in energy. The second of these steps is rate determining and hence intersystem crossing is an irreversible process, i.e. vibrational relaxation within the triplet

Figure 9Arrhenius Plots for Methyl-9-anthroate in
Methanol, Ethanol and p-Dioxane

Typical Arrhenius plots for methyl-9-anthroate are presented. This figure shows three of the solvents used: methanol, ethanol and p-dioxane. The good linearity observed indicates that intersystem crossing is the only non-radiative pathway depopulating S_1 . The slopes of these plots are directly proportional to the activation energy.



manifold is also much faster than the transition from the singlet to the triplet state and hence also from the triplet to the singlet state. Because of this, the overall rate for the process in which a molecule in the 0th vibrational level of S_1 end up in the triplet manifold is given by the product of k_{isc} and the relative population of the S_1 vibrational level, $S_1(v_1)$, isoenergetic with T_2 (equation 10).

$$\text{Rate}_{isc} = k_{isc} S_1(v_1) \quad (10)$$

The k_{isc} in equation 10 is the same as the k_{NR} given in equation 2. Hence, for a molecule in a given solvent, it is $S_1(v_1)$ which changes and accounts for the temperature dependence of ϕ_f and for a molecule in different solvents but at the same temperature it is both k_{isc} and $S_1(v_1)$ which will determine the value of ϕ_f since in general both of these terms will change with changes in the S_1 - T_2 energy gap.

The quantum yield of intersystem crossing may be defined as the ratio of rate constant for intersystem crossing and the sum of the processes deactivating S_1 (equation 11).

$$\phi_{isc} = k_{isc} / (k_{isc} + k_f) \quad (11)$$

Since intersystem crossing and fluorescence are the only two processes which depopulate S_1 , the sum of their quantum yields must be 1 (equation 12). Substituting equation 12 into

$$\phi_{isc} + \phi_f = 1 \quad (12)$$

equation 11 and rearranging, one can express k_{isc} in terms of k_f and ϕ_f (equation 13).

$$k_{isc} = (k_f/\phi_f) - k_f \quad (13)$$

Table V gives k_{isc} values for 2-COOMe and 9-COOMe in the solvents indicated^{at 22°C}. These values are calculated assuming a k_f of $5.9 \times 10^7 \text{ sec}^{-1}$ for 9-COOMe and $4.4 \times 10^7 \text{ sec}^{-1}$ for 2-COOMe. The k_{isc} values for 2-COOMe show a general increase with decreasing solvent polarity while those for 9-COOMe show a drastic increase with increasing solvent polarity. The results given in the table for 2-COOMe can be explained in terms of an energy level diagram where T_2 remains fairly constant with solvent polarity and slightly higher in energy than S_1 which undergoes a marked decrease in energy with increasing solvent polarity. With increasing solvent polarity, previous work has shown⁽⁸⁾ that the S_1-T_2 energy gap in 2-COOMe increases and thus we would expect that the overall rate of intersystem crossing would become smaller. This has been found to be the case. The k_{isc} results given in the table for 9-COOMe, however, cannot be explained in terms of this simple model. To gain insight into the unexpected behavior of 9-COOMe, it is necessary to understand the relative effects of solvent polarity on the S_1-T_2 energy gap and on ϕ_f and τ_a .

Figure 10 shows a plot of ϕ_f for 9-COOMe in the solvents indicated versus solvent polarity as measured by the empirical $E_T(30)$ solvent polarity scale. As the figure indicates, the quantum yields in non-aromatic solvents fall on a straight line and the quantum yields in aromatic solvents fall on another line. This effect may be due to the previously described $\pi-\pi$

TABLE V

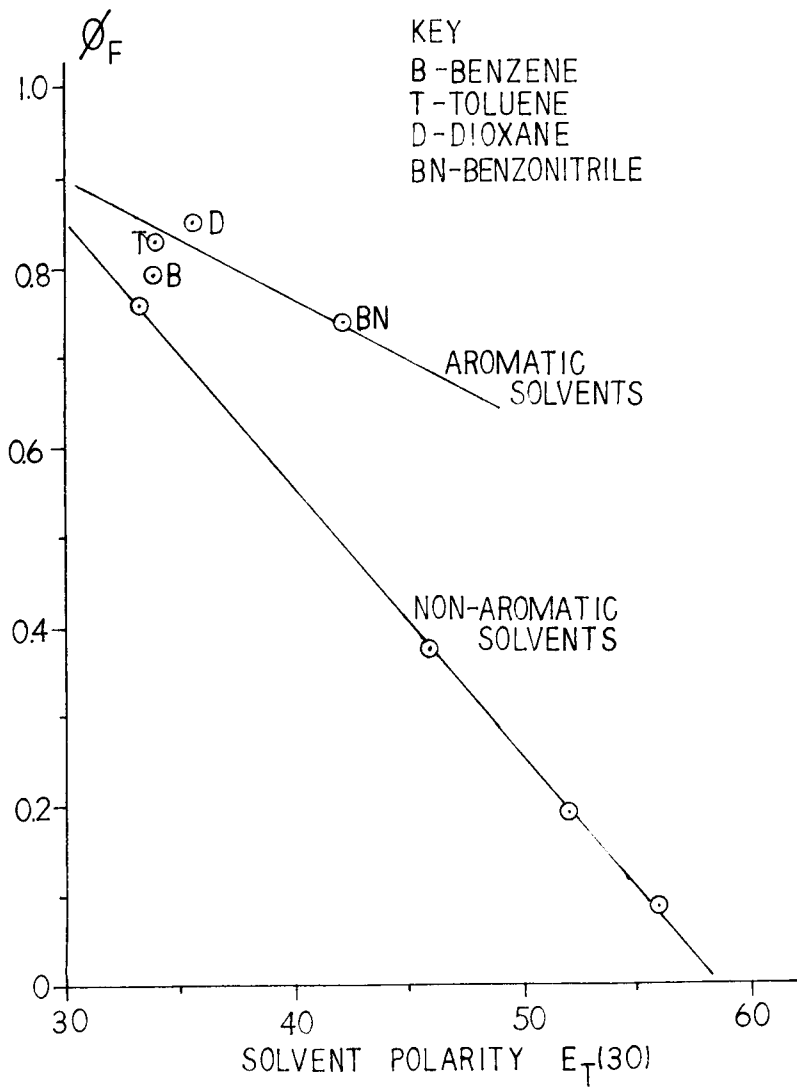
Intersystem Crossing Rate Constants for 2-COOMe and 9-COOMe
in Various Polar and Non-polar Solvents at 22°C.

| <u>Compound</u> | <u>Solvent</u> | <u>k_{isc} (10^7sec^{-1})</u> |
|--------------------|------------------|---|
| Methyl-9-anthroate | Methanol | 66±3 |
| | Ethanol | 28±1 |
| | Acetonitrile | 9.6±0.4 |
| | Benzonitrile | 2.0±0.1 |
| | Toluene | 1.7±0.1 |
| | Benzene | 1.3±0.1 |
| | Cyclohexane | 1.9±0.1 |
| | p-Dioxane | 1.0±0.1 |
| Methyl-2-anthroate | Benzonitrile | 0.49±0.02 |
| | Benzene | 1.1±0.1 |
| | Toluene | 1.7±0.1 |
| | Cumene | 2.1±0.1 |
| | Acetonitrile | 0.38±0.01 |
| | Ethanol | 0.49±0.02 |
| | Trifluoroethanol | 0.43±0.02 |
| | p-Dioxane | 0.90±0.03 |
| | Cyclohexane | 5.0±0.2 |
| | Hexane | 9.4±0.3 |

Figure 10

Fluorescence Quantum Yield as a function of Solvent Polarity
for Methyl-9-anthroate

Fluorescence Quantum Yields for methyl-9-anthroate decrease rapidly with increasing solvent polarity with behaviors noted for this molecule in aromatic and non-aromatic solvents.

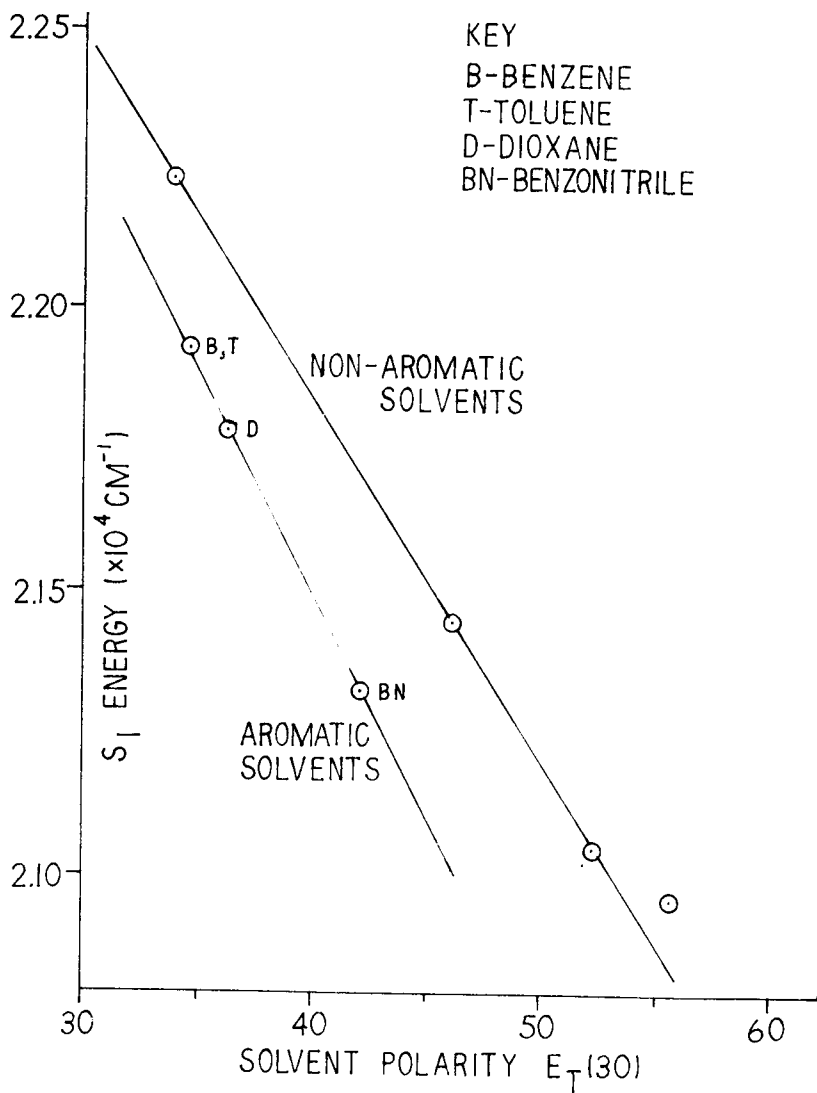


solute-solvent interaction. It is interesting to note that p-dioxane shows behavior typical of aromatic solvents and that toluene lies about midway between the lines for aromatic and non-aromatic solvents. The behavior of 9-COOMe in toluene may be due to the fact that the methyl group offers steric hindrance to the π - π interaction of toluene and 9-COOMe and hence these interactions are smaller making the behavior in toluene less aromatic-like and more non-aromatic. It is interesting to note that depending on the slope of the line that can be drawn for ϕ_f in the aromatic solvents, the two lines intersect at a ϕ_f between 0.95 and 1.0 in extremely low polarity solvents.

Figure 11 gives a plot of the S_1 energies of 9-COOMe in the solvents indicated. Amazing linearity is noted for all solvents except methanol. Again, the behavior of 9-COOMe in aromatic solvents is decidedly different from its behavior in non-aromatic solvents. As indicated in the figure, the S_1 energies in aromatic solvents are redshifted to the extent of 200-300 cm^{-1} compared to nonaromatic solvents of the same polarity. This effect is clearly seen as a result of solute-solvent π - π interactions. It is well known from Hückel-Molecular Orbital theory that increasing the π conjugation in a conjugated system of atoms increases the energy of the highest occupied molecular orbital (HOMO) and decreases the energy of the lowest unoccupied molecular orbital (LUMO). Hence the energy of transitions from the HOMO to the LUMO decreases with increasing conjugation. Because no π interactions are possible

Figure 11Methyl-9-anthroate S_1 Energy vs. Solvent Polarity

The S_1 energy for methyl-9-anthroate shows a monotonic decrease with increasing solvent polarity. Separate lines are observed for this molecule in aromatic and non-aromatic solvents with the aromatic line being red-shifted with respect to the non-aromatic line. Amazing linearity for the S_1 energies in both types of solvent are noted.



with non-aromatic solvents, the redshifted S_1 energies of 9-COOMe in aromatic solvents can be attributed to an increase in conjugation due to the weak $\pi-\pi^*$ solute-solvent interactions. An alternative way of looking at this is to say that these $\pi-\pi^*$ interactions offer additional stabilization to S_1 causing a redshift in S_1 . These two descriptions actually say the same thing since stabilization of S_1 amounts to decreasing the energy gap between HOMO and LUMO. The observation that the slope of the line for 9-COOMe in aromatic solvents is greater than that for 9-COOMe in non-aromatic solvents is an indication that something more than just solvent polarity is determining the energy of S_1 among the aromatic solvents. This may indicate the presence of added stabilization in a more polar aromatic solvent "encounter complex" due to excited state dipole-induced dipole interactions. It is known that excited state rotation of the carboxyl group of 9-COOMe occurs giving essential double bond character to the bond between the carboxyl carbon and the parent ring. As a result a charge separation occurs in which the carboxyl oxygen carries the negative charge and the carbon in the 10 position of the ring carries the positive charge and the entire molecule is in a nearly planar geometry allowing for a greater possibility of $\pi-\pi^*$ interactions than in the non-coplanar ground state. In encounter complexes where benzene and toluene are the solvent, it is expected that because of the polarizability of aromatic solvents, the only stabilization that will occur in addition to the $\pi-\pi^*$

interaction itself will be due to a very weak excited state dipole-induced dipole interaction. With a more polar solvent such as benzonitrile, there is a greater opportunity for dipole-dipole stabilization in addition to π - π stabilization. Solvent effects are also expected to contribute an added degree of stabilization of S_1 for 9-COOMe in benzonitrile when molecules in the solvent cage of the equilibrium excited state have their negative dipoles near the positive end of the of the molecule in its excited state and vice versa. Thus we would expect that the more polar the aromatic solvent, the greater will be the induced dipole and solvent effects on S_1 energies. In polar aromatic solvents, the linearity of the S_1 energy-solvent polarity plot may be lost and the line may actually begin to curve downward as charge transfer effects begin to become of importance. It is interesting that p-dioxane again shows pseudo-aromatic behavior. Apparently the lone pairs of electrons on the two oxygens may have an effect similar to the π electrons of an aromatic solvent. A similar effect has been observed with lone pairs of electrons on nitrogen. In a study on the geometric requirements for excimer formation, Taylor⁽³⁰⁾ concluded that the lone pair of electrons on the nitrogen in 3,5-di-tert-butyl-N,N-dimethylaniline were responsible for fluorescence quenching of S_1 in pyrene. Because of the steric hindrance offered by the tert-butyl groups on the benzene ring, a sandwich structure for excimer formation was ruled out. Rather, quenching was ascribed to the much

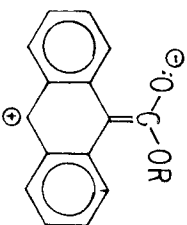
easier approach of the lone pair of electrons on the nitrogen to the π electrons of pyrene. It is believed that a similar phenomenon is being observed in the case of p-dioxane exciplex formation with 9-COOMe. The observation that a pair of electrons has the same effect on the red-shifting of S_1 energies is substantiated by Taylor's observation that fluorescence quenching in pyrene is just as effective when the quencher is N,N-dimethylaniline (sandwich exciplex formation possible) as it is when the quencher is 3,5-di-tert-butyl-N,N-dimethylaniline where the sandwich structure is not likely to occur. In other words, lone pairs and π electrons can have similar effects on S_1 quenching and in this work on S_1 stabilization. Additional evidence for solvent exciplex formation comes from temperature dependent data of the S_1 energy of 9-COOMe in benzonitrile. We have observed a 200 cm^{-1} blue shift in the S_1 energy of this system when increasing the temperature from 0°C to 90°C indicating the "breaking" up of the complex as described. Figure 12 gives a summary of the hypothesized geometric requirements for the weak exciplex formation of 9-COOMe in p-dioxane and aromatic solvents. Note the distinction between sandwich exciplexes which are possible in aromatic solvents and lone pair exciplex formation which is possible in p-dioxane. The slopes of the S_1 energy versus solvent polarity line for 9-COOMe in aromatic and non-aromatic solvents are -76 cm^{-1} and -60 cm^{-1} , respectively.

Figure 13 shows a plot of E_a versus solvent polarity for

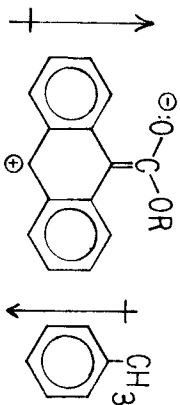
Figure 12

Electronic Distribution in the Excited State (S_1) of 9-COOMe
and Structure of the Solvent Cage and Exciplex

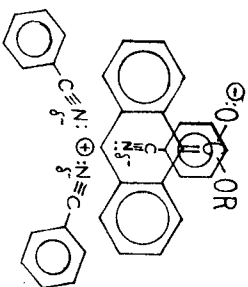
The S_1 excited state shows a dipole moment directed along the short axis of the molecule and pointing towards the carboxyl group. Charge separation exists with the negative charge on the carboxyl oxygen and the positive charge on the 10 position of the ring. Weak exciplex formation reduces the energy of S_1 by 200-300 cm^{-1} . "Sandwich" exciplex formation is aided by dipole-dipole interactions within the excited state complex and between solute and solvent in reducing the energy of S_1 even further in polar aromatic molecules such as benzonitrile. Lone pair exciplex formation may occur when the solvent is p-dioxane.



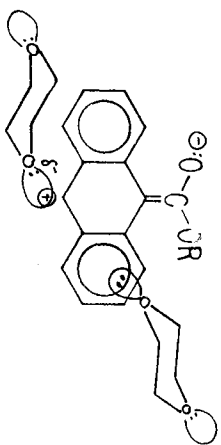
EXCITED STATE (S_1) CHARGE
DISTRIBUTION IN 9-COOME



EXCITED STATE DIPOLE AND
INDUCED DIPOLE IN TOLUENE
EXCIPLEX



EXCIPLEX FORMATION IN BENZONITRILE
PARTIAL STRUCTURE OF SOLVENT CAGE

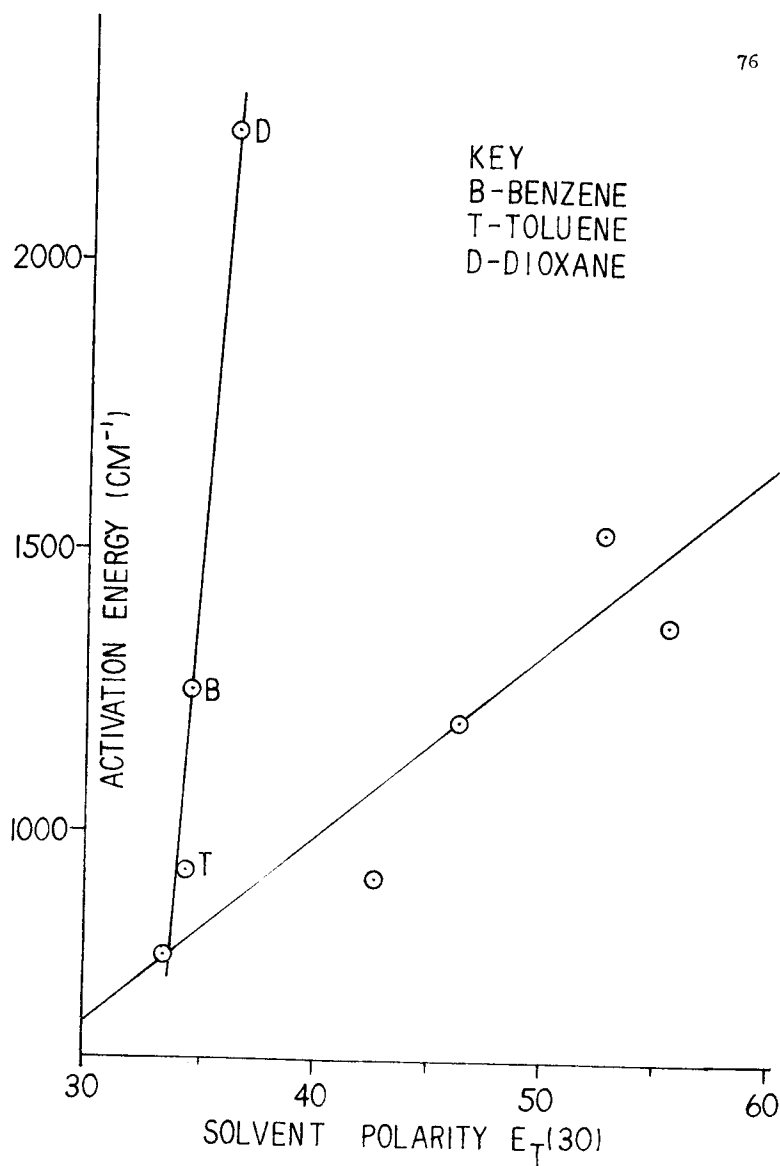


LONE PAIR SOLVENT INTERACTION AND
EXCIPLEX FORMATION IN DIOXANE

Figure 13

Activation Energy as a Function of Solvent Polarity
for Methyl-9-anthroate

Activation energies for methyl-9-anthroate are plotted as a function of solvent polarity. The majority of solvents fall on somewhat of a straight line with positive slope indicating that the S_1-T_2 gap is increasing with increasing solvent polarity. The reason why the activation energy in benzene and p-dioxane fall off the line is not clear.



9-COOMe in the solvents indicated. Values for E_a were given in Table IV. Again, separate behavior is observed for 9-COOMe in aromatic and non-aromatic solvents although the meaning of this behavior is not clear. Since non-linearity is observed in the Arrhenius plots in aromatic solvents (Figure 7), activation energies were picked from the slope of that portion of the curve where linearity was maintained, usually at the lower temperature end of the plot. In all solvents but benzene and p-dioxane, 9-COOMe exhibits an increase in activation energy with increasing solvent polarity. This is to be expected if S_1 is decreasing with increasing solvent polarity and intersystem crossing occurs to a triplet level which is relatively unaffected by solvent polarity. The anomalous behavior of E_a in benzene and p-dioxane has not been explained.

Figure 14 shows a plot of $S_1 + E_a$ versus solvent polarity for 9-COOMe in the solvents indicated. As expected a difference is seen in the behavior of 9-COOMe in aromatic and non-aromatic solvents although this difference is not as clear cut as before. The sum of S_1 and E_a may be interpreted as the energy of T_2 . In non-aromatic and aromatic solvents T_2 red-shifts with increasing solvent polarity although in non-aromatic solvents the degree to which T_2 redshifts over the solvent polarity range is considerably less than that in aromatic solvents. An indication of the degree to which T_2 drops in energy in these solvents is expressed by the slopes of the lines given in the figure which are -82 cm^{-1} and -30 cm^{-1} in aromatic and non-

TABLE VI

$S_1 + E_a$ for methyl-9-anthroate and methyl-2-anthroate in various polar, non-polar and aromatic solvents.

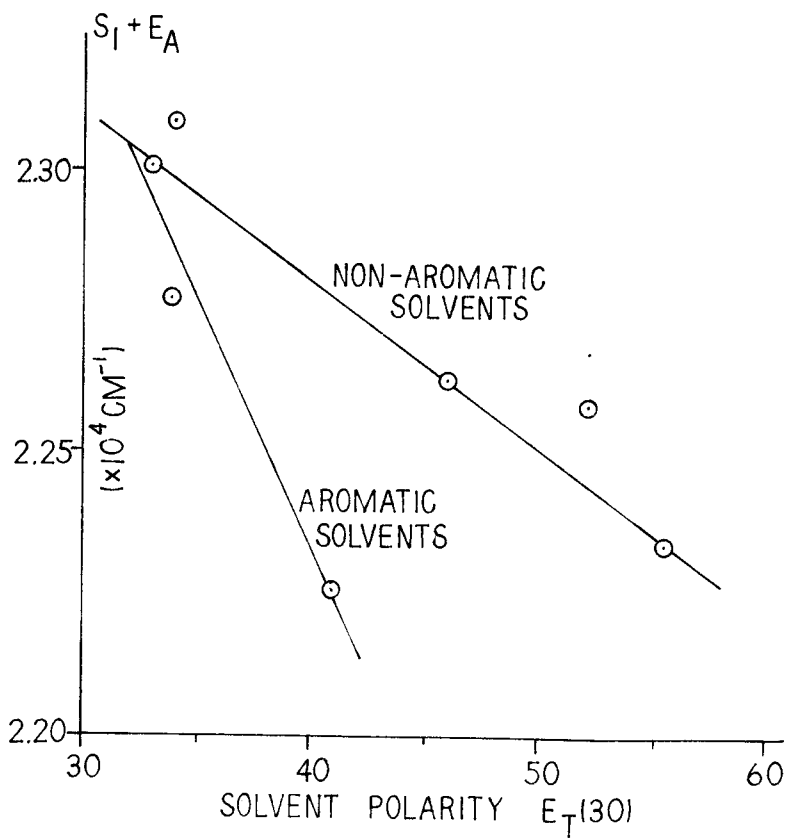
| <u>Compound</u> | <u>Solvent</u> | <u>$S_1 + E_a$ (cm⁻¹)</u> |
|--------------------|------------------|---|
| Methyl-9-anthroate | Methanol | 22,340 ± 200 |
| | Ethanol | 22,570 ± 110 |
| | Acetonitrile | 22,619 ± 140 |
| | Benzonitrile | 22,252 ± 230 |
| | Toluene | 22,764 ± 220 |
| | Benzene | 23,086 ± 295 |
| | Cyclohexane | 23,010 ± 170 |
| Methyl-2-anthroate | Benzonitrile | 24,840 ± 360 |
| | Benzene | 25,620 ± 170 |
| | Toluene | 25,350 ± 80 |
| | Cumene | 25,380 ± 120 |
| | Acetonitrile | 25,225 ± 360 |
| | Ethanol | 24,680 ± 360 |
| | Trifluoroethanol | TIF* |
| | p-Dioxane | 25,760 ± 200 |
| | Cyclohexane | 25,940 ± 60 |
| | Hexane | 25,860 ± 50 |

*Temperature Independent Fluorescence

Figure 14

S_1 Energy + E_a for 9-COOMe as a Function
Solvent Polarity

The sum of the S_1 energy and activation energy for 9-COOMe in various solvents is plotted as a function of solvent polarity. This sum gives an estimate of the T_2 energy in these solvents. In general, the T_2 energy decreases with increasing solvent polarity, however, separate behaviors are observed in non-aromatic and aromatic solvents with the T_2 energy being more affected by solvent polarity in the latter type of solvent.



aromatic solvents, respectively, which indicates that T_2 is slightly more affected than S_1 in the former solvents and much less affected in the latter solvents by solvent polarity. The relatively smaller dependence of T_2 on solvent polarity than S_1 in non-aromatic solvents is supportive of our hypothesis. However, the surprising effect of the dependence of T_2 in aromatic solvents on solvent polarity is consistent with all the results presented on aromatic data and is helpful in explaining the curvature of the Arrhenius plots of 9-COOMe in benzene, toluene and benzonitrile. These plots, which are shown in Figure 7, indicate that E_a increases with increasing temperature. This seems to be inconsistent with the data that the S_1 energy for 9-COOMe in benzonitrile increases with increasing temperature, i.e. E_a should decrease if T_2 remains fairly constant. However, as explained previously T_2 is more sensitive to the presence of aromatic solvents than S_1 . Hence when the temperature is increased and the complex dissociates as indicated by the blue-shifting of S_1 , T_2 should blue-shift as well, but should do so to a greater degree than S_1 with the result that the S_1 - T_2 energy gap for 9-COOMe in benzonitrile should increase with increasing temperature. Thus an increase in E_a is expected with increasing temperature, which was found to be the case. The Arrhenius plots for 9-COOMe in benzene and toluene show only slight curvature toward higher E_a with increasing temperature. Presumably, this is a result of the fact that complexing is weaker in these solvents

because of smaller excited state dipole-induced dipole interactions than those present in benzonitrile.

Figure 15 shows a plot of E_a versus S_1 energy for 9-COOMe in the solvents indicated. All the points except that for benzene fall on a straight line. A decrease in E_a is noted with increasing S_1 energy as expected. If the line is extended to zero activation energy, the intercept corresponds to an S_1 energy of about $23,700\text{ cm}^{-1}$ which is presumably the energy of T_2 . The slope of the line is -0.5 which indicates that S_1 is increasing twice as fast as E_a is decreasing which is a restatement of T_2 blue-shifting with decreasing solvent polarity.

Aromatic data have been collected for 2-COOMe (Figure 16). The S_1 energies decrease with increasing solvent polarity with S_1 energies for 2-COOMe in aromatic solvents being correspondingly lower than the S_1 energy in a non-aromatic solvent of similar polarity. The slopes of the aromatic and non-aromatic lines given in the figure are approximately equal, being -71 and -76 cm^{-1} , respectively. As described previously, the corresponding slopes for 9-COOMe were -76 and -60 cm^{-1} . Hence, it appears that S_1 energies in both molecules are affected to a similar extent by solvent polarity indicating that the first excited singlet in these molecules are of approximately the same polarity. It would be difficult to push this argument too far because of the sparsity of data which has been collected for each line. It appears that the behavior

Figure 15

Activation Energy vs. S_1 Energy for 9-COOMe

The activation energy is plotted vs. the singlet energy for methyl-9-anthroate in a series of solvents. Such a plot shows a fairly linear decrease in activation energy with increasing singlet energy. The slope of the line is less than one indicating that T_2 is blueshifting with increasing S_1 energy and decreasing solvent polarity.

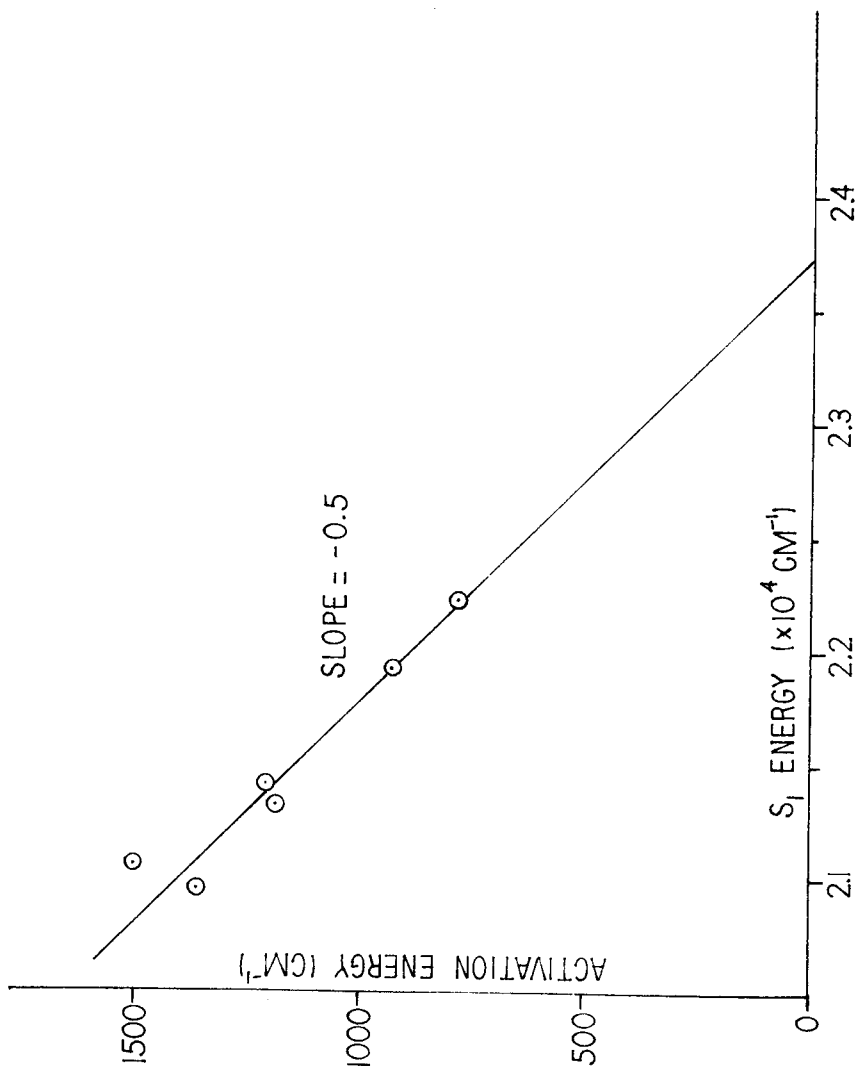
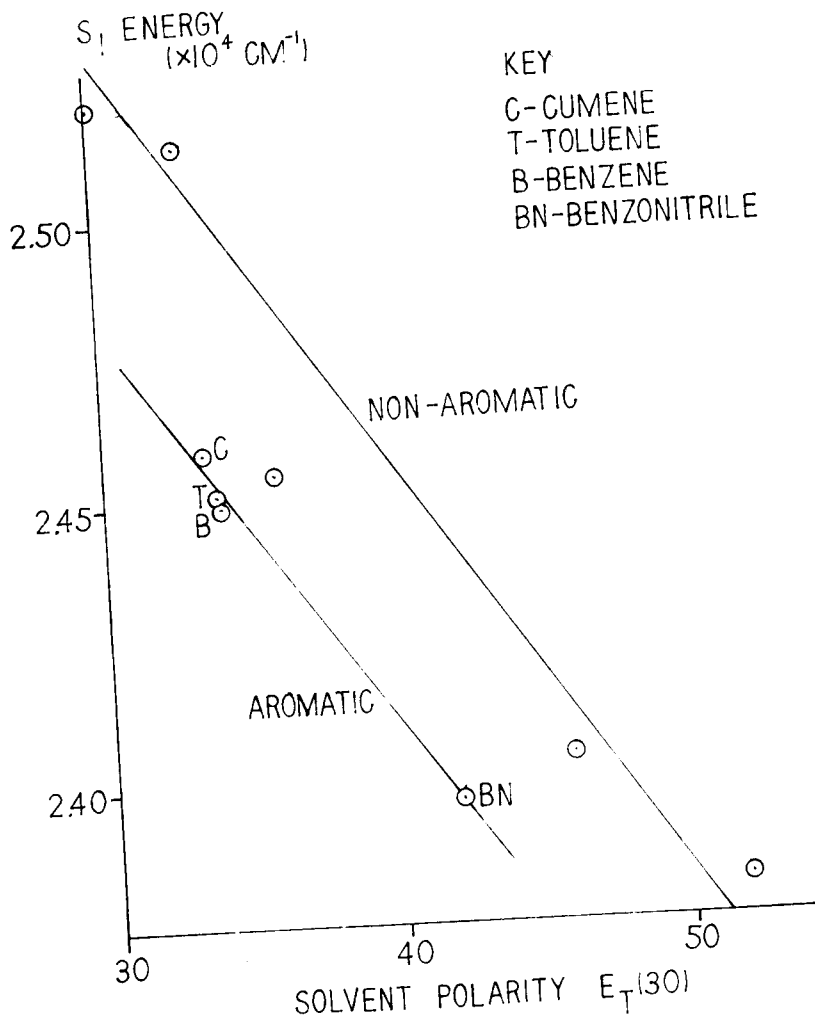


Figure 16

S_1 Energy vs. Solvent Polarity for Methyl-2-anthroate

When S_1 energies for methyl-2-anthroate are measured as a function of solvent polarity, it is found that increasing solvent polarity decreases this energy with respect to the ground state. Again, separate behaviors are observed for the S_1 energy of this molecule in non-aromatic and aromatic solvents with the energy in the latter solvent type being red-shifted with respect to non-aromatic solvents.



of 9-COOMe in non-aromatic solvents may be different from 2-COOMe in these solvents but more data must be collected before any conclusions may be drawn. Mixed solvent experiments, which are described later, may yield some valuable information here.

Because the 9-position of the ring is more electron rich than the 2-position and because the $S_0 \rightarrow S_1$ transition is short axis polarized, it is expected that the first excited singlet of 9-COOMe is a more polar state than that of 2-COOMe. However, it is entirely possible that excited state rotation in 9-COOMe is not complete and that the conformation of the molecule in S_1 is not as planar as expected. The main steric hindrance to excited state rotation comes from the interaction of the hydrogens in the 1- and 8-positions and the carboxylic oxygens. Because of incomplete rotation, there is less double bond character between the carboxyl group and the ring and hence less negative charge on the carbonyl oxygen resulting in a less polar excited state than expected. The steric hindrance of the 9-carboxyl group may also inhibit the most energetically stable solvent cage from forming about 9-COOMe. Since the S_1 energies for this molecule are less than that of 2-COOMe in all solvents, it seems that ground state destabilization is greater in the former than in the latter because of excited state rotation and the possibility that the solvent cage is not allowed to assume the most favorable configuration about 9-COOMe. Hence, for the reasons indicated above, the position of the carboxyl

group seems to have only a minimal effect in determining S_1 polarities.

The singlet energies of 2-COOMe in benzene, toluene and cumene are of interest. A decided blue-shift occurs with an increase in the size of the substituent on the benzene ring. This has been attributed to an increase in intermolecular distance between solute and solvent in exciplex formation. Steric inhibition prevents a close approach of the solvent because of the increasing size of the substituent resulting in poorer π - π overlap between solute and solvent.

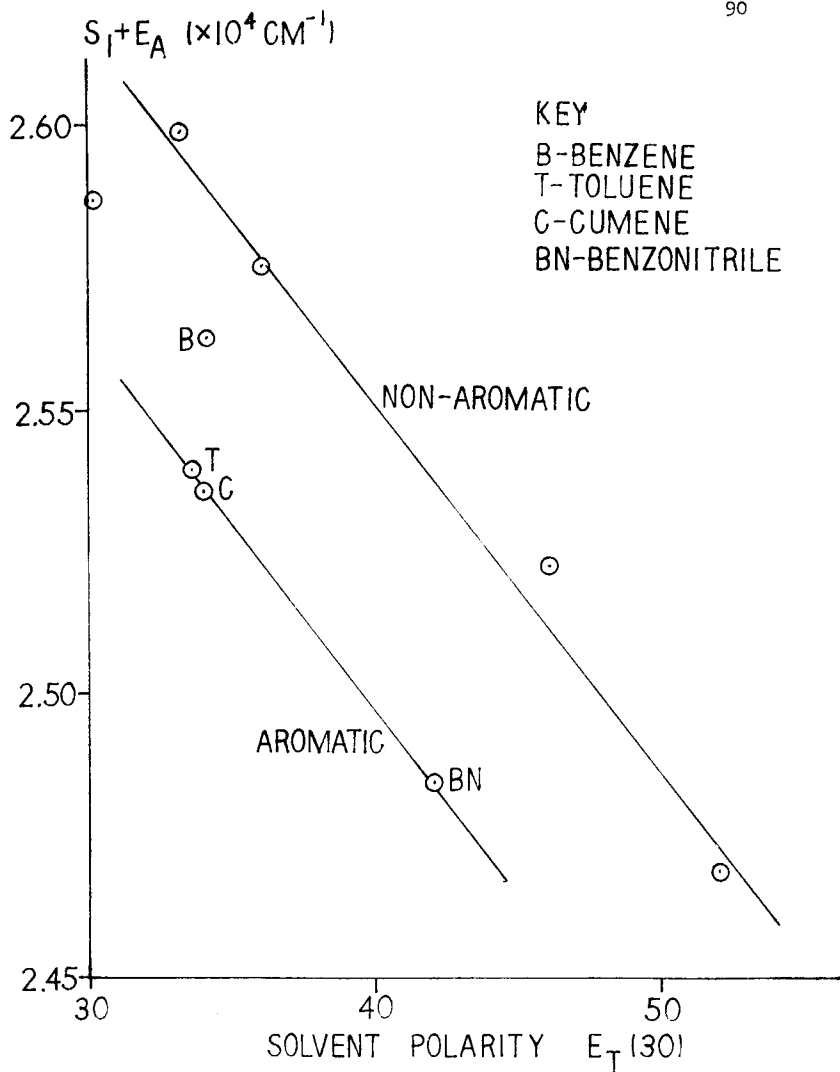
Activation energies for 2-COOMe were summarized in Table IV. Values in non-aromatic solvents were obtained in a previous work⁽⁸⁾ and corrected for a change in our reference quantum yield. Values in aromatic solvents were performed in this work. The sum of E_a and S_1 should yield a minimum energy for T_2 . These values are summarized in Table VI and plotted versus solvent polarity in Figure 17. A certain degree of linearity is observed in this plot. Similar data presented by Hawkins⁽⁸⁾ for 2-COOMe in non-aromatic solvents show excellent linearity. The fact that the benzonitrile and ethanol values happen to fall on the line may be attributed to luck since the ϕ_f values for 2-COOMe in these solvents are quite high making the determination of E_a very difficult and subject to large errors.

Different lines are observed for ν_2 versus solvent polarity depending on the solvent type. The slopes of these lines are similar being -64 cm^{-1} and -65 cm^{-1} in aromatic and non-

Figure 17

$S_1 + E_a$ vs. Solvent Polarity for Methyl-2-anthroate

The sum of the singlet energy and activation energy for methyl-2-anthroate in various solvents are plotted versus solvent polarity. This sum is an estimate of the T_2 energy and shows a fairly linear decrease with increasing solvent polarity. Two lines are observed for the triplet energy, one corresponding to that in non-aromatic solvents and the other to aromatic solvents. As expected, the triplet energy in aromatic solvents is red-shifted with respect to that in non-aromatic solvents.



aromatic solvents, respectively. Because of the sparsity of data, it is difficult to attribute too much meaning to the values of the slopes other than that they are similar. Again, it appears that T_2 is more affected by aromatic solvents than is S_1 . This can be seen by noting that in Figure 16, S_1 is red-shifted by about 450 cm^{-1} in aromatic solvents whereas T_2 is red-shifted by about 550 cm^{-1} as shown in Figure 17. Finally, the S_1 energy of 2-COOMe in benzonitrile has been observed to blue-shift by 150 cm^{-1} when the temperature was increased from room temperature to 90°C . In addition, the Arrhenius plot displayed non-linearity, i.e. an increase in E_a was observed with increasing temperature. These findings may be explained in a manner wholly similar to that given for 9-COOMe in benzonitrile.

In summary, then, our original hypothesis that T_2 is much less responsive to environmental effects than S_1 seems to have support for 9-COOMe only in non-aromatic solvents and previous work⁽⁸⁾ has indicated that this is also the case for 2-COOMe in non-aromatic solvents. Our energy level scheme for non-aromatic cases is that of an increasing S_1 - T_2 energy gap with increasing solvent polarity, S_1 and T_1 separated by between 7500 cm^{-1} and $10,000\text{ cm}^{-1}$. The overall rate of inter-system crossing which is thermally assisted will be dependent on the S_1 - T_2 energy gap. Hence, ϕ_f should increase, k_{isc} decrease and E_a increase with increasing solvent polarity.

Unfortunately, the simple model above does not predict

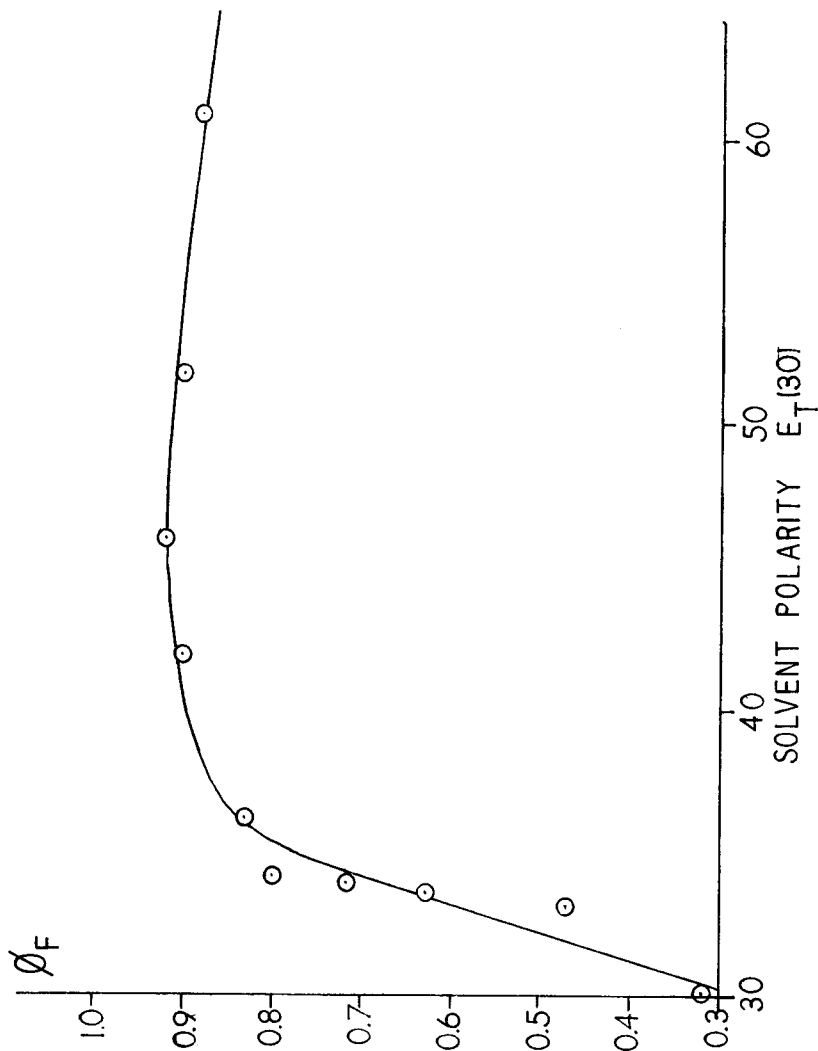
reality very well. This model predicts the behavior of 2-COOMe fairly well in low and moderately polar solvents. Figure 18 shows that ϕ_f for 2-COOMe passes through a maximum and shows a decrease in highly polar solvents. Figure 10 shows a general decrease in ϕ_f for 9-COOMe with increasing solvent polarity and Table V indicates that k_{isc} increases remarkably with increasing polarity and hence energy gap. These findings are completely opposite to what the simple energy level diagram would predict. We, therefore, propose a more sophisticated model to explain the anomalous behavior of ϕ_f and k_{isc} in 9-COOMe in all solvents and 2-COOMe in highly polar solvents based on a similar model found in the literature.

We propose that a vibrational structuring of the Franck-Condon factor for intersystem crossing occurs when the lowest excited singlet and accepting triplet lie close in energy, usually less than about 1500 cm^{-1} . Tanaka and Osugi⁽⁵⁾ have proposed a similar vibrational structuring of the Franck-Condon factor when S_1 lies slightly above T_2 but have not extended their argument for the case when S_1 is only slightly below T_2 , assuming that in this latter case k_{isc} will decrease monotonically and rather rapidly with increasing S_1 - T_2 energy gap. Our results indicate this is not the case. When the Franck-Condon factor shows a vibrational structure, the rate of non-radiative transitions may show considerable variation with a small perturbation of the system such as occurs with changes in solvent. Both 9-COOMe and 2-COOMe are in this category

Figure 18

ϕ_f vs. Solvent Polarity for Methyl-2-anthroate

The fluorescence quantum yield of methyl-2-anthroate shows a maximum with increasing solvent polarity which is marked by a steep rise at low polarity and a slow decline at higher polarity.



since as the activation energy values point out S_1 is within 1500 cm^{-1} of T_2 in most solvents.

Equation 2 gives an expression for the rate constant of a non-radiative transition in terms of an electronic matrix, the density of states and the Franck-Condon factor. This expression may be used to describe the rate constant of inter-system crossing. Although the nature of the electronic matrix is not clear, it seems that it will not be affected by small changes in energy⁽⁵⁾ between S_1 and T_2 . Sharf and Silbey⁽³¹⁾ have also shown that the density of final states does not depend strongly on the energy gap. They have pointed out that the coupling of T_2 with the vibrationally excited levels of T_1 will constitute a continuous final state in the triplet manifold near the 0th vibrational level of T_2 . This lends support to our hypothesis that crossing occurs to 0th vibrational level of T_2 for reasons explained previously. It is often shown that the Franck-Condon factor between the lowest vibrational levels of S_1 and T_2 will depend greatly on the S_1 - T_2 energy gap. Evidence for this comes in the high degree of vibrational structure in the absorption and fluorescence spectra of anthracene and many of its derivatives with accompanying increases and decreases in the Franck-Condon factor. Other theoretical treatments summarized in the literature⁽⁵⁾ have indicated the importance of the dependence of the Franck-Condon factor on energy gap when the gap is small.

These factors have been calculated for the S_1 - T_2 energy

gap in anthracene where S_1 lies 650 cm^{-1} above T_2 , and they show a considerable dependence on changes in this gap. In particular maxima and minima are noted with the Franck-Condon factor varying from .2 to near 1. Anthracene exhibits vibrational progressions of 1400 cm^{-1} and 400 cm^{-1} in its absorption and fluorescence spectra. The 400 cm^{-1} progression is also seen in the phosphorescence spectrum of anthracene⁽³²⁾ which is not too surprising since these transitions (fluorescence and phosphorescence) involve S_0 , a common state. It is interesting that the triplet-triplet absorption spectrum for anthracene does not exhibit these 400 cm^{-1} progressions⁽⁵⁾ which are thought to correspond to a totally symmetric skeletal bending vibration.

The 1400 and 400 cm^{-1} progressions found in anthracene's absorption and fluorescence spectra have also been found in this work in the absorption spectra of 9-COOMe, 9-COOBe, and 9-COOPE. We, therefore, believe that the vibrational structure of the Franck-Condon factor for the S_1 - T_2 energy gap in anthracene as calculated by Tanaka is appropriate here. It appears that because of the similarity of the vibrational progressions, which arise from skeletal bending modes of the parent ring, the qualitative features of the Franck-Condon factor-energy gap curve proposed in the literature will apply to our system. However, since S_1 lies below T_2 in the molecules examined in this work, we propose, contrary to Tanaka's hypothesis, that the Franck-Condon factor does not show a monotonic

decrease as S_1 drops farther below T_2 , but shows a vibrational structure when S_1 is below T_2 and a monotonic decrease only when the energy gap becomes larger. Figure 18 shows an estimate of the variation in the Franck-Condon factor with energy gap. Note that after an initial decrease in the curve, the Franck-Condon factor passes through a maximum and then shows a monotonic decrease. The anomalous results for ϕ_f and k_{isc} for 9-COOMe can be explained by assuming that the S_1 - T_2 gaps in different solvents lie on the rising (positive slope) portion of the curve. Methyl-9-anthroate in non-polar solvents would be placed on the lower portion of this part of the curve since the energy gap is smaller (as evidenced by smaller E_a 's and larger S_1 energies), while 9-COOMe in polar solvents would be located on the upper portion of the curve with positive slope (as evidenced by larger E_a 's and smaller S_1 energies). Hence, an increase in the Franck-Condon factor is observed with increasing solvent polarity and increasing energy gap. Since the electronic matrix element and density of final states is relatively constant over the small energy changes (1500 cm^{-1}), k_{isc} also shows an increase with increasing solvent polarity as our results point out. Because k_{isc} competes with fluorescence, the lifetime of fluorescence and hence quantum yield of fluorescence shows a corresponding decrease as our results also point out.

The fact that ϕ_f for 2-COOMe passes through a maximum, may also be qualitatively explained by a variation in the

Franck-Condon factor. However, it seems more likely that the decreasing portion of the quantum yield curve for 2-COOMe may be better explained by crossing from S_1 to T_1 . Evidently, increasing solvent polarity has decreased the S_1 energy level to a point where intersystem crossing to the first triplet has begun to take on importance. Increases in solvent polarity lower the S_1 energy with respect to T_1 and because of the smaller energy gap between these states, the probability of transition rises. Presumably intersystem crossing is also occurring to the higher triplet, T_2 . The evidence for this comes from the temperature dependence of the quantum yields for 2-COOMe in the solvents that are on the falling part of the quantum yield curve. The fraction of the molecules which proceed by this latter route decreases fairly rapidly since intersystem crossing to the higher triplet is described by the Arrhenius equation and follows an exponential decrease with increasing S_1 - T_2 energy gap. This can be seen experimentally from the fact that 2-COOMe in acetonitrile which is at the maximum in the curve shows a substantial dependence of ϕ_f on temperature while ϕ_f for this molecule in trifluoroethanol is temperature independent. Therefore, at low solvent polarity, crossing to T_2 is the major non-radiative pathway whereas at higher polarity crossing to the lower triplet becomes of importance.

The vibrational structuring of the Franck-Condon factor has been successfully applied to the explanation of other

complicated intersystem crossing behavior⁽⁵⁾ brought about by temperature, pressure, deuteration and substitution perturbations. It is clear that this theory, although slightly more complicated than the simple "energy gap law", describes more accurately the intersystem crossing process and may be used to clear up some of the ambiguities, uncertainties and seeming contradictions which appear in the literature⁽²³⁾.

An alternative explanation of the anomalous results for ϕ_f and k_{isc} for 9-COOme involves solvent induced puckering of the anthracene ring of 9-COOme in S_1 . Much of the conjugation of the ring is lost in its lowest excited state, as shown in Figure 10. The anthracene ring essentially becomes a system of two independent benzene rings because conjugation is lost in the middle ring. As a result one might expect less rigidity in the excited state resulting in puckering of the anthracene ring by the solvent cage. A treatment of the mechanism of S_1-T_X intersystem crossing based on solvent induced puckering of aromatic hydrocarbons has been found in the literature. As is well known, the spin-orbit interactions between singlet and triplet π, π^* states is weak. Enhancement of intersystem crossing can be brought about by mixing σ, π^* and π, π^* states of the same multiplicity. This is due to the fact that spin-orbit interaction between these states is quantum mechanically more favorable than spin-orbit interaction between π, π^* states. The question which remains is which mode of ring distortion will bring about the proper mixing of

states. El-Sayed⁽³³⁾ concludes that out-of-plane distortion is more favorable than in-plane distortion in bringing about enhancement of the intersystem crossing process. The exact role of solvent in bringing about distortion of the ring and hence enhancement of k_{isc} is not clear at present but is probably a function of solvent polarity such that increasing solvent polarity would increase puckering of the anthracene ring and enhance the probability of intersystem crossing. This would have to be the case since the experimental data indicate as shown in Table V that k_{isc} increases with increasing solvent polarity for 9-COOMe. Further investigations into the effect of solvent puckering are needed as they may throw additional light on the details of the mechanism of intersystem crossing.

FUTURE WORK

One of the possible routes for this project is the performance of mixed solvent studies. Mixed solvents have the advantage of providing a nearly continuous range of solvent polarity. S_1 energies should be measured in mixed aromatic and mixed non-aromatic solvents such as benzene-benzonitrile and acetonitrile-ethanol. One has to make the assumption that solvent polarity varies linearly with changes in the mixed solvent composition since $E_T(30)$ values are not known here. This should yield information on the relative polarities of the first excited singlet in 2-COOMe and 9-COOMe and perhaps tell us something about the effect of the position of the carboxyl group on S_1 or the geometry of the excited state.

Since the details of the suspending of solutes in polymethylmethacrylate without catalysts have been worked out, phosphorescence measurements should be done on anthracene, 2-COOMe and 9-COOMe. The phosphorescence intensity in these molecules is expected to be extremely low, so that a special photomultiplier sensitive in the red must be used since phosphorescence lies to the red of fluorescence. The details of such a photomultiplier arrangement are being worked on at present. This would be an invaluable piece of information since it would give the energy of T_1 and hence a knowledge of the S_1 - T_1 gap in 2-COOMe in polar solvents where intersystem crossing is believed to occur to T_1 .

Intersystem crossing to T_1 can be best checked through deuteration studies. Since the S_1-T_1 energy gap is fairly large, C-H vibrations will be important in the non-radiative transition to T_1 . Therefore, deuteration of the compound to be studied should change the **photophysics** of this molecule if the above non-radiative transition is significant. Since only ring C-H vibrations are important in the transition, only the anthracene portion of the molecule need be deuterated. One way of accomplishing this is to synthesize the perdeutero 9- and 2-anthracene-carboxylic acids through treatment with D_2SO_4 and D_2O and esterification of the acid with CH_3OH . The quantum yield of these compounds in a variety of solvents can then be determined and compared with the compounds that were not deuterated. If the quantum yields are comparable, then crossing to T_1 is not important, however, if the quantum yield is greater in the perdeutero compound then it can be concluded that the S_1-T_1 transition is significant or less likely internal conversion to S_0 is occurring.

Finally, exciplex formation should be further examined. The room temperature fluorescence spectra of 9-COOFE and 9-COOBe in cyclohexane have not shown evidence of intramolecular exciplex formation. This may be due to the polarity of the solvent and to the fact that at room temperature the ester part of the molecule possesses too much thermal energy for the benzene ring to sit over the top of the anthracene ring in a sandwich type of conformation. Therefore, to look for

evidence of exciplex formation, it is proposed that the fluorescence spectra of these molecules be taken in ethanol or some other suitable H-bonding solvent which forms a glass at 77°K. Evidence of intramolecular exciplex formation should be seen as a long wavelength peak not present in 9-COOMe at 77°K and as a peak whose intensity should change with changes in temperature in the fluid solvent.

REFERENCES

1. Ralph S. Becker, "Theory and Interpretation of Fluorescence and Phosphorescence", Wiley-Interscience, New York, N.Y., (1969) Chapter 1.
2. U. Wild, H. Griesser and V.D. Tuan, Chem. Phys. Letters, 41, 450 (1972).
3. Reference 1, at pp. 104-109.
4. M.F. Thomaz and M. Barradas, Chem. Phys. Letters, 17, 360 (1972).
5. F. Tanaka and J. Osugi, Chem. Phys. Letters, 27, 133 (1969).
6. F. Tanaka and J. Osugi, Chem. Phys. Letters, 29, 1279-1283 (1973).
7. W.R. Ware and B.A. Baldwin, J. Chem. Phys. 43, 1194 (1965).
8. William Hawkins, Undergraduate Thesis, Chem. Dept., Union College, 1976.
9. Thomas Matthews, Undergraduate Thesis, Chem. Dept., Union College, 1975.
10. Reference 1, at pg. 96.
11. J. Laposa, G. Lim and R. Kellogg, J. Chem. Phys., 42, 3025 (1965).
12. Reference 1, at pg. 143.
13. J. Birks, "Photophysics of Aromatic Molecules", Wiley-Interscience, London, 1970, 256-252.
14. E. Lim and J. Laposa, J. Chem. Phys., 41, 3257 (1964).
15. R.W. Shaw and M. Nicol, Chem. Phys. Letters, 39, 111, (1969).
16. R.G. Bennett and P.J. McCartin, J. Chem. Phys., 44, 1969 (1966).
17. A.R. Horrocks, T. Bedinger and F. Wilkinson, Photochemistry and Photobiology, 6, 21-28 (1967).
18. Synthesized by Dr. T.C. Werner at Union College

19. R.C. Parish and L.M. Stock, *J. Org. Chem.*, 927, March 1965.
20. "Dictionary of Organic Compounds, 4th ed.", Oxford University Press, New York, 1, 252 (1965).
21. R. Torrisi, Undergraduate Thesis, Chem. Dept., Union College, 1976.
22. A.J. Gordon and R.A. Ford, "The Chemist's Companion", John Wiley and Sons, New York, N.Y., 1972, pg. 214.
23. T.C. Werner, unpublished data.
24. T.C. Werner and D.M. Hercules, *J. Phys. Chem.*, 73, 2005, (1969).
25. Lin-Cowan and Schmiegell, *J. Phys. Chem.*, 79, 1975
26. Huber, Morriss and Mahaney, *J. Phys. Chem.*, 80, 969 (1976).
27. *J. Phys. Chem.*, 46, 4511 (1967).
28. J. Fernandez and R.S. Becker, *J. Chem. Phys.*, 31, 467, (1959).
29. Same as 25.
30. G.N. Taylor, E.A. Chandross and A.H. Schiebel, *J. Amer. Chem. Soc.*, 96, 2693 (1974).
31. B. Scharf and R. Silbey, *J. Chem. Phys.*, 44, 1969 (1966).
32. M.R. Padhye, S.E. McGlynn and M. Kasha, *J. Chem. Phys.*, 24, 588 (1956).
33. M.A. El-Sayed, W.R. Moomaw and J.B. Chodak, *Chem. Phys. Letters*, 20, 11 (1973).